View metadata, citation and similar papers at core.ac.uk

brought to you by CORE

provided by Victoria University Eprints Repository

Received: 13 January 2016 | Accepted: 1 March 2017

DOI: 10.1002/hyp.11163

WILEY

RESEARCH ARTICLE

Cokriging for enhanced spatial interpolation of rainfall in two Australian catchments

Sajal Kumar Adhikary[1,2] | Nitin Muttil[1,2] | Abdullah Gokhan Yilmaz[3]

[1] College of Engineering and Science, Victoria University, P.O. Box 14428, Melbourne, Victoria 8001, Australia

[2] Institute for Sustainability and Innovation, Victoria University, P.O. Box 14428, Melbourne, Victoria 8001, Australia

[3] College of Engineering, University of Sharjah, P.O. Box 27272, Sharjah, United Arab Emirates

Correspondence
Sajal Kumar Adhikary, College of Engineering and Science, Victoria University, Footscray Park Campus, P.O. Box 14428, Melbourne, Victoria 8001, Australia.
Email: sajal.adhikary@live.vu.edu.au

Abstract

Rainfall data in continuous space provide an essential input for most hydrological and water resources planning studies. Spatial distribution of rainfall is usually estimated using ground-based point rainfall data from sparsely positioned rain-gauge stations in a rain-gauge network. Kriging has become a widely used interpolation method to estimate the spatial distribution of climate variables including rainfall. The objective of this study is to evaluate three geostatistical (ordinary kriging [OK], ordinary cokriging [OCK], kriging with an external drift [KED]), and two deterministic (inverse distance weighting, radial basis function) interpolation methods for enhanced spatial interpolation of monthly rainfall in the Middle Yarra River catchment and the Ovens River catchment in Victoria, Australia. Historical rainfall records from existing rain-gauge stations of the catchments during 1980–2012 period are used for the analysis. A digital elevation model of each catchment is used as the supplementary information in addition to rainfall for the OCK and kriging with an external drift methods. The prediction performance of the adopted interpolation methods is assessed through cross-validation. Results indicate that the geostatistical methods outperform the deterministic methods for spatial interpolation of rainfall. Results also indicate that among the geostatistical methods, the OCK method is found to be the best interpolator for estimating spatial rainfall distribution in both the catchments with the lowest prediction error between the observed and estimated monthly rainfall. Thus, this study demonstrates that the use of elevation as an auxiliary variable in addition to rainfall data in the geostatistical framework can significantly enhance the estimation of rainfall over a catchment.

KEYWORDS

cross-variogram model, digital elevation model, kriging with an external drift, ordinary cokriging, positive-definite condition, variogram model

1 | INTRODUCTION

Rainfall data provide an essential input for many hydrological investigations and modelling tasks. Accuracy of various hydrological analyses such as water budget analysis, flood modelling, climate change studies, drought management, irrigation scheduling, and water management greatly depends on the correct estimation of the spatial distribution of rainfall (Delbari, Afrasiab, & Jahani, 2013; Moral, 2010). This usually requires a dense rain-gauge network with a large number of stations (Adhikary, Muttil, & Yilmaz, 2016a). However, the rain-gauge network is often sparse in the field because the number of stations in a network is often restricted by economic, logistics, and geological factors (Goovaerts, 2000). As a result, point rainfall data are generally accessible from a limited number of stations. These limitations increase the need for using suitable spatial estimation methods to obtain the spatial distribution of rainfall and generate rainfall map from the point rainfall values. Moreover, the network is often not deployed on a regular grid and rainfall data may not be available in the target location where it is most required (Adhikary et al., 2016a). In such cases, spatial interpolation plays a vital role to simulate rainfall in areas with no stations based on the observed rainfall values in the surrounding areas.

This is an open access article under the terms of the Creative Commons Attribution-NonCommercial-NoDerivs License, which permits use and distribution in any medium, provided the original work is properly cited, the use is non-commercial and no modifications or adaptations are made.
© 2017 The Authors. Hydrological Processes Published by John Wiley & Sons Ltd.

Several interpolation methods have been frequently employed to interpolate rainfall data from rain-gauge stations and produce the spatial distribution of rainfall over a catchment. Examples of such methods range from simple conventional (e.g., Thiessen polygons [Thiessen, 1911], isohyet mapping [ASCE, 1996], simple trend surface interpolation [Gittins, 1968]), and deterministic methods (i.e., inverse distance weighting (IDW; ASCE, 1996), radial basis function (RBF; Di Piazza, Conti, Noto, Viola, & Loggia, 2011) to complex stochastic or geostatistical methods (i.e., ordinary kriging [OK], ordinary cokriging [OCK] and kriging with an external drift [KED; Goovaerts, 2000]). Although the conventional and deterministic methods have been improved over time, their limitations continue to exist. These limitations have been described elaborately in Goovaerts (2000) and Teegavarapu and Chandramouli (2005).

Geostatistical methods have been shown superior to the conventional and deterministic methods for spatial interpolation of rainfall (Goovaerts, 1997; Isaaks & Srivastava, 1989). Several studies have reported that rainfall is generally characterised by a significant spatial variation (e.g., Delbari et al., 2013; Lloyd, 2005). This suggests that interpolation methods, which are explicitly able to incorporate the spatial variability of rainfall into the estimation process should be employed. In view of that, kriging has become the most widely used geostatistical method for spatial interpolation of rainfall. The ability of kriging to produce spatial predictions of rainfall has been distinguished in many studies (e.g., Adhikary et al., 2016a; Goovaerts, 2000; Jeffrey, Carter, Moodie, & Beswick, 2001; Lloyd, 2005; Moral, 2010; Yang, Xie, Liu, Ji, & Wang, 2015). The major advantage of kriging is that it takes into account the spatial correlation between data points and provides unbiased estimates with a minimum variance. The spatial variability in kriging is quantified by the variogram model that defines the degree of spatial correlation between the data points (Webster & Oliver, 2007).

Another key advantage of kriging over the conventional and deterministic methods is that while providing a measure of prediction standard error (also called kriging variance), it is capable of complementing the sparsely sampled primary variable, such as rainfall by the correlated densely sampled secondary variable, such as elevation to improve the estimation accuracy of primary variable (Goovaerts, 2000; Hevesi, Istok, & Flint, 1992). This multivariate extension of kriging is referred to as the cokriging method. The standard form of cokriging is the OCK method, which usually reduces the prediction error variance and specifically outperforms kriging method if the secondary variable (i.e., elevation) is highly correlated (correlation coefficient higher than .75) with the primary variable (i.e., rainfall) and is known at many more points (Goovaerts, 2000). The KED is another commonly applied cokriging method, which can incorporate the exhaustive secondary variable (i.e., elevation) to give an enhanced estimation of rainfall when dealing with a low-density rain-gauge network. Thus, cokriging including the OCK and KED methods has been the increasing preferred geostatistical methods all over the word. As highlighted by Goovaerts (2000) and Feki, Slimani, and Cudennec (2012), rainfall and elevation tend to be related because of the orographic influence of mountainous topography. Therefore, topographic information such as the digital elevation model (DEM) can be used as a convenient and valuable source of secondary data for the OCK and KED methods. The efficacy of incorporating elevation into the interpolation procedure for enhanced estimation of rainfall has been highlighted in many studies across the world (e.g., Di Piazza et al., 2011; Feki et al., 2012; Hevesi et al., 1992; Lloyd, 2005; Martínez-cob, 1996; Moral, 2010; Phillips, Dolph, & Marks, 1992; Subyani & Al-Dakheel, 2009).

A wide variety of spatial interpolation methods have been developed for the interpolation of spatially distributed point rainfall values. However, it is often challenging to distinguish the best interpolation method to estimate the spatial distribution of rainfall for a particular catchment or study area. The reason is that the performance of an interpolation method depends on a number of factors such as catchment size and characteristics, sampling density, sample spatial distribution, sample clustering, surface type, data variance, grid size or resolution, quality of auxiliary information to be used as well as the interactions among these factors. Moreover, it is unclear how the aforementioned factors affect the performance of the spatial interpolation methods (Dirks, Hay, Stow, & Harris, 1998; Li & Heap, 2011). Hence, the best interpolation method for a particular study area is usually established through the comparative assessment of different interpolation methods (e.g., Delbari et al., 2013; Dirks et al., 1998; Goovaerts, 2000; Hsieh, Cheng, Liou, Chou, & Siao, 2006; Mair & Fares, 2011; Moral, 2010). The comparison among different interpolation methods is made through a validation procedure. The interpolation method that provides better results with lower bias and higher accuracy in rainfall estimation is identified as the best interpolation method.

In the past, many studies have been devoted to the comparison and evaluation of different deterministic and geostatistical interpolation methods in a range of different regions and climates around the world. Dirks et al. (1998) compared four spatial interpolation methods using rainfall data from a network of 13 rain-gauges in Norfolk Island concluding that kriging provided no substantial improvement over any of the simpler Thiessen polygon (TP), IDW, or areal-mean methods. Goovaerts (2000) employed three multivariate geostatistical methods (OCK, KED, simple kriging with varying local means [SKVM]), which incorporate a DEM as secondary variable and three univariate methods (OK, TP, and IDW) that do not take into account the elevation for spatial prediction of monthly and annual rainfall data available at 36 rain-gauge stations. The comparison among these methods indicated that the three multivariate geostatistical methods gave the lowest errors in rainfall estimation. Martínez-cob (1996) compared OK, OCK, and modified residual kriging to interpolate annual rainfall and evapotranspiration in Aragón, Spain. The results indicated that OCK was superior for rainfall estimation, reducing estimation error by 18.7% and 24.3% compared with OK and modified residual kriging, respectively. Hsieh et al. (2006) evaluated OK and IDW methods using daily rainfall records from 20 rain-gauges to estimate the spatial distribution of rainfall in the Shih-Men Watershed in Taiwan. The results demonstrated that IDW produced more reasonable representations than OK. Moral (2010) compared three univariate kriging (simple kriging [SK], universal kriging, and OK) with three multivariate kriging methods (OCK, SKVM, and regression kriging) to interpolate monthly and annual rainfall data from 136 rain-gauges in Extremadura region of Spain. The results showed that multivariate kriging outperformed univariate kriging and among multivariate kriging, SKVM and regression kriging performed better than OCK.

Ly, Charles, and Degré (2011) used IDW, TP, and several kriging methods to interpolate daily rainfall at a catchment scale in Belgium.

The results indicated that integrating elevation into KED and OCK did not provide improvement in the interpolation accuracy for daily rainfall estimation. OK and IDW were considered to be the suitable methods as they gave the smallest error for almost all cases. Mair and Fares (2011) compared TP, IDW, OK, linear regression, SKVM to estimate seasonal rainfall in a mountainous watershed concluding that OK provided the lowest error for nearly all cases. They also found that incorporating elevation did not improve the prediction accuracy over OK for the correlation between rainfall and elevation lower than 0.82. Delbari et al. (2013) used two univariate methods (IDW and OK), and four multivariate methods (OCK, KED, SKVM, and linear regression) for mapping monthly and annual rainfall over the Golestan Province in Iran. They reported that KED and OK outperformed all other methods in terms of root mean square error (RMSE). Jeffrey et al. (2001) derived a comprehensive archive of Australian rainfall and climate data using a thin plate smoothing spline to interpolate daily climate variables and OK to interpolate daily and monthly rainfall. The aforementioned studies on spatial interpolation of rainfall indicate that each method has its advantages and disadvantages and thus performs in a dissimilar way for different regions. There is no single interpolation method that can work well everywhere (Daly, 2006). Therefore, the best interpolator for a particular study area or catchment should essentially be achieved through the comparative assessment of different interpolation methods.

To date, many studies have been conducted on spatial interpolation of rainfall at a regional and national scale in Australia (Gyasi-Agyei, 2016; Hancock & Hutchinson, 2006; Hutchinson, 1995; Jeffrey et al., 2001; Johnson et al., 2016; Jones, Wang, & Fawcett, 2009; Li & Shao, 2010; Woldemeskel, Sivakumar, & Sharma, 2013; Yang et al., 2015). However, none of these studies was conducted at a local or catchment scale. Likewise, elevation and rainfall relations locally have been relatively little studied in Australia and no such studies have been undertaken specifically within the Yarra River catchment and the Ovens River catchment in Victoria, Australia. Sharma and Shakya (2006) highlighted that any analysis of hydroclimatic variables should be carried out at the local scale rather than at a large or global scale because of the variations of hydroclimatic situations from one region to another. Therefore, the main aim of this study is to assess if relatively more complex geostatistical interpolation methods that take into account the elevation and rainfall relation provide any benefits over simpler methods for enhanced estimation of rainfall within the Yarra River catchment and the Ovens River catchment in Victoria, Australia. The specific focus is to evaluate the effectiveness of the cokriging methods including OCK and KED that make use of elevation as a secondary variable over those methods including OK, IDW, and RBF that do not make use of such information to estimate the spatial distribution of rainfall within the catchment. This study is expected to provide an important contribution towards the enhanced estimation of rainfall in the aforementioned two Australian catchments using the cokriging methods by incorporating elevation as an auxiliary variable in addition to rainfall data. One specific contribution of this paper is in explaining how rainfall varies with elevation from catchment to catchment.

The Yarra River catchment and the Ovens River catchment in Victoria are selected for this study because they are two important water resources catchments in Australia in terms of water supply and agricultural production (Adhikary, Yilmaz, & Muttil, 2015; EPA Victoria, 2003; Schreider, Jakeman, Pittock, & Whetton, 1996; Yu, Cartwright, Braden, & de Bree, 2013). The Yarra River catchment is a major source of water for more than one third of Victoria's population in Australia (Barua, Muttil, Ng, & Perera, 2012). Although the catchment is not large with respect to other Australian catchments, it produces the fourth highest water yield per hectare of the catchment in Victoria (Adhikary et al., 2015). There are seven storage reservoirs in the catchment that supports about 70% of drinking water supply in Melbourne city (Barua et al., 2012). The Ovens River catchment is another important source of water in northeast Victoria, which forms a part of the Murray-Darling basin (Yu et al., 2013). The Ovens River is considered one of the most important tributaries of the Murray-Darling Basin due to the availability of sufficient volume of water with acceptable quality and its good ecological condition. The average annual flow of the river constitutes approximately 7.3% of the total flow of the state of Victoria (Schreider et al., 1996). The catchment contributes approximately 14% of Murray-Darling basin flows in spite of its relatively small catchment area of less than 1% of the total Murray-Darling basin area (EPA Victoria, 2003; Yu et al., 2013). Thus, both the catchments have significant contribution towards the sustainable development of Victoria's economy. However, high rainfall variation and diverse water use activities in these catchments has complicated the water management tasks, which has further created strong burden on the water managers and policy makers for effective water resources management. Therefore, enhanced estimation of rainfall and its spatial distribution is important, which could be beneficial for effective water supply and demand management, and sustainable agricultural planning in both the catchments.

The rest of the paper is arranged as follows. First, a brief description of the study area and data used are presented, which is followed by the detailed description of the methodology adopted in this study. The results are summarized next, and finally, the conclusions drawn from this study are presented.

2 | STUDY AREA AND DATA USED

2.1 | The study area

This study considers two catchments in Victoria as the case study area, which includes the Middle Yarra River catchment and Ovens River catchment in south-eastern Australia. Figure 1 shows the approximate location of the case study area. The Yarra River catchment is located in northeast of Melbourne covering an area of 4,044 km^2. The water resources management is an important and multifaceted issue in the Yarra River catchment because of its wide range of water uses as well as its downstream user requirements and environmental flow provisions (Barua et al., 2012). The catchment significantly contributes to the water supply in Melbourne and has been playing an important role in the way Melbourne has been developed and grown (Adhikary et al., 2015). The Yarra River catchment consists of three distinctive subcatchments including Upper, Middle, and Lower Yarra segments based on different land use activities (Barua et al., 2012). This study concentrates on the Middle segment of the Yarra River catchment, which forms part of the case study area in Figure 1. The Upper Yarra segment includes mainly the forested and mountainous areas with minimum human settlement, which is mainly used as a closed water supply

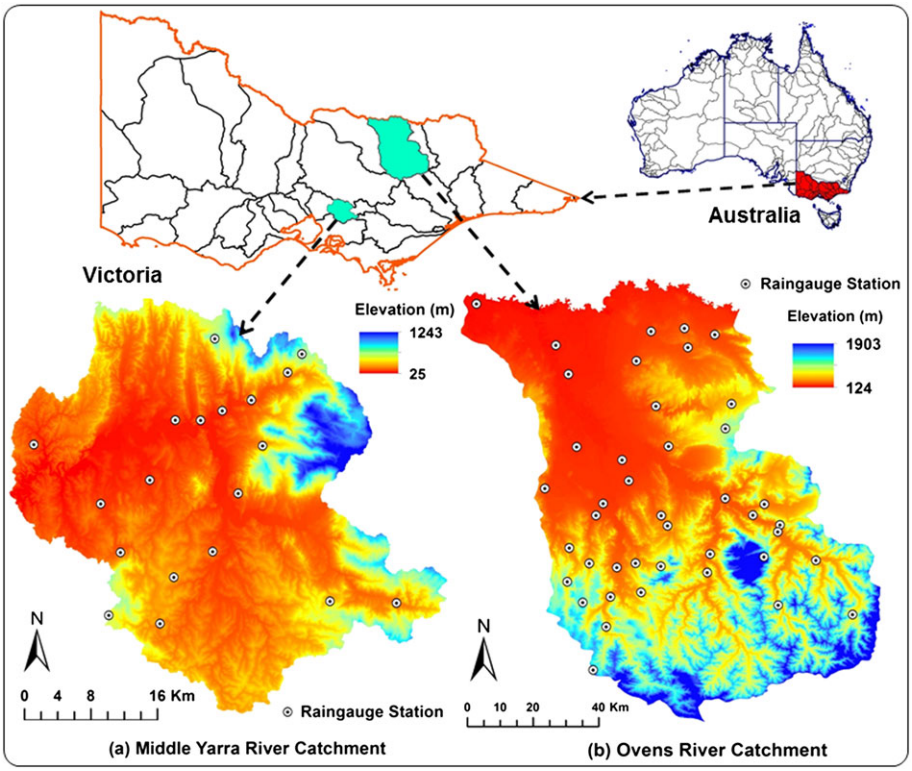

FIGURE 1 Location and topography of (a) Middle Yarra River catchment and (b) Ovens River catchment in Victoria with existing rain-gauge stations

catchment for Melbourne and has been reserved for more than 100 years for water supply purposes. The Middle Yarra segment, starting from the Warburton Gorge to Warrandyte Gorge, is notable as the only part of the catchment with an extensive flood plain, which is mainly used for agricultural activities. The Lower Yarra segment of the catchment, which is located downstream of Warrandyte, is mainly characterized by the urbanized floodplain areas of Melbourne city (Adhikary, Muttil, & Yilmaz, 2016b). Most of the land along rivers and creeks in the middle and lower segments has been cleared for the agricultural or urban development (Barua et al., 2012; Melbourne Water, 2015).

Rainfall varies significantly through different segments of the Yarra River catchment. The mean annual rainfall varies across the catchment from 600 mm in the Lower Yarra segment to 1,100 mm in the Upper Yarra segment (Daly et al., 2013). The Middle Yarra segment (part of the case study area in Figure 1) covers an area of 1,511 km^2 and consists of three storage reservoirs. Decreasing rainfall patterns in the catchment will reduce the streamflows, which in turn will lead to the reduction in reservoir inflows and hence impact the overall water availability in the catchment. Moreover, the reduced streamflows may cause increased risk of bushfires. Conversely, increasing rainfall patterns and the occurrence of extreme rainfall events (as reported in Yilmaz and Perera [2014] and Yilmaz, Hossain, and Perera [2014]) will result in excess amount of streamflows that may cause flash floods in the urbanized lower segment and makes it vulnerable and risk-prone. The urbanized lower part of the catchment is also dependent on the water supply from the storage reservoirs mainly located in the middle and upper segments of the catchment (Adhikary et al., 2015). Therefore, accurate spatial distribution of rainfall in the middle and upper segments of the catchment could be useful for accurate estimation of future streamflows for optimal reservoir operation and effective flood control in the urbanized lower part.

The Ovens River catchment in northeast Victoria is also considered as a part of the case study area in this study, which is shown in Figure 1. The catchment covers an area of 7,813 km^2 (Yu et al., 2013), which extends from the Great Dividing Range in the south to the Murray River in the north, with the Yarrawonga Weir forming the downstream boundary. It is considered to be one of the least modified catchments within the Murray-Darling basin. The catchment contributes approximately 14% to the average flows of the Murray River in spite of its relatively small size (0.75 percent of the total Murray-Darling Basin area; EPA Victoria, 2003; Yu et al., 2013). The Ovens River is the main river in the catchment, which originates on the northern edges of the Victorian Alps and flows in a north-westerly direction until its junction with the Murray River near Lake Mulwala. The riverine plains and alluvial flats are primarily cleared for agricultural use, while the hills and mountains are covered by forests with native plant species (Yu et al., 2013). Total average water use in the catchment is about 30,000 million litres per year, 64% of which is diverted from the Ovens River and its tributaries. A major part of this water use is irrigation, which constitutes more than 16,000 million litres annually (Schreider et al., 1996). The river itself provides natural conditions suitable for many significant native fish species, particularly the endangered Murray Cod (EPA Victoria, 2003). Thus, the catchment is considered to be important, not only at a regional scale, but also at the national scale in terms of its water supply volume for domestic and agricultural production, and high environmental value.

The climate of the Ovens River catchment varies considerably with topography and elevation (Yu et al., 2013). The average annual rainfall varies from 1,127 mm in the Alpine region at Bright to 636 mm on the alluvial plains in Wangaratta with most rainfall

occurring in winter months (Yu et al., 2013). Approximately 45% of the annual rainfall occurs during the winter (June to September) whereas the summer is warm and dry. Winter snowfalls are common at altitudes above 1,000 m (EPA Victoria, 2003). Therefore, enhanced estimation of rainfall and its spatial distribution could be useful for the effective management of water supply and agricultural activities in the catchment.

2.2 | Data used

In this study, historical rainfall data from existing rain-gauge stations in the Middle Yarra River catchment and the Ovens River catchment (Figure 1) for 1980–2012 period are considered. There are 19 rain-gauge stations in the Middle Yarra River catchment, whereas the Ovens River catchment includes 42 rain-gauge stations operated by the Australian Bureau of Meteorology. Daily rainfall data are collected from the Scientific Information for Land Owners climate database (http://www.longpaddock.qld.gov.au/silo/) and compiled to generate monthly and annual rainfall, which are then used for the analysis. Summary statistics of monthly rainfall data are given in Table 1. The annual average rainfall in the Middle Yarra River catchment for the aforementioned period varies from 710 mm to 1422 mm with a mean value of 1082 mm. The southern and south-eastern part experiences the highest rainfall, whereas the lowest rainfall occurs in the north-western part in the study area. September is the wettest month (rainfall amount equals to 112.5 mm) with the highest variation in rainfall. The driest month is February (rainfall amount equals to 56.4 mm) with the second highest variability. On the other hand, the annual average rainfall for the same period in the Ovens River catchment varies from 231 to 2,473 mm with a mean value of 913 mm. The wettest month is July (rainfall amount equals to 112.9 mm) with the highest variability and February (rainfall amount equals to 51.3 mm) appears to be the driest month with the third highest variation in rainfall.

For the OCK analysis, a DEM of both the catchments with 10 m resolution (shown in Figure 1) is collected from the Geoscience Australia. The elevation of the Middle Yarra River catchment varies from 25 m (lowest-mainly in central, north-western, and western part) to 1,243 m (highest-mainly in northern, north-eastern, and eastern part) with a mean elevation of 621 m above mean sea level. Whereas, the elevation of the Ovens River catchment varies from 124 m (lowest-mainly in the upper north-western part) to 1903 m (highest-mainly in the lower southern, south-eastern and eastern part) with a mean elevation of 874 m above mean sea level. Monthly and annual rainfall generally tend to increase with the higher elevations caused by the orographic effect of mountainous terrain (Goovaerts, 2000). Several studies have revealed that rainfall usually shows good correlation with elevation. For example, Goovaerts (2000) showed that a good to significant correlation exists between the monthly rainfall and elevation,

TABLE 1 Summary statistics for monthly rainfall data of Middle Yarra River catchment and Ovens River catchment

Month	Mean (mm)	Minimum (mm)	Maximum (mm)	Standard deviation (mm)	Correlation coefficient (versus elevation)[a]
Middle Yarra River catchment					
January	67.3	1.8	201.4	31.23	0.79
February	56.4	0.0	269.5	53.40	0.69
March	66.3	9.2	217.8	36.89	0.77
April	84.7	15.2	246.0	45.81	0.74
May	88.3	10.2	239.7	42.47	0.67
June	106.4	13.8	300.2	46.18	0.70
July	102.1	17.9	303.9	48.95	0.73
August	108.6	21.1	289.7	50.67	0.72
September	112.5	25.3	350.3	56.98	0.67
October	101.6	4.0	333.9	50.86	0.69
November	96.1	15.3	258.7	47.60	0.77
December	91.3	8.2	301.2	52.88	0.74
Ovens River catchment					
January	55.8	0.0	364.7	51.41	0.49
February	51.3	0.0	421.9	65.66	0.26
March	53.7	0.3	418.1	51.01	0.49
April	54.5	1.0	234.6	38.63	0.72
May	74.6	2.0	360.7	56.71	0.61
June	95.4	1.4	457.0	62.99	0.65
July	112.9	6.0	622.4	71.92	0.60
August	105.2	5.8	468.0	68.94	0.61
September	86.3	5.2	484.1	55.44	0.65
October	73.4	0.1	410.8	61.61	0.67
November	73.6	0.6	290.8	47.70	0.68
December	64.1	0.2	374.6	54.79	0.68

[a]Linear correlation coefficient between rainfall and elevation data.

which varies from .33 to .83. Subyani and Al-Dakheel (2009) found that good correlation ranging from .34 to .77 exists between seasonal rainfall and elevation in the Southwest Saudi Arabia. Moral (2010) identified a good correlation ranging from .33 to .67 between monthly and annual rainfall and elevation in the southwest region of Spain.

As can be seen in Table 1, the correlation coefficient (CC) between the monthly average rainfall and elevation for the Middle Yarra River catchment varies from .67 to .79, where 8 months have the CC values greater than .70. This indicates that a strong correlation exists between the monthly rainfall and elevation in the catchment, suggesting that elevation may enhance the monthly rainfall estimates when used as a secondary variable in the OCK analysis. On the contrary, the CC between the monthly average rainfall and elevation for the Ovens River catchment varies from .26 to .72, where 6 months exhibit the CC values higher than .65. Apart from the driest month of February, the correlation ranges from .49 to .72 in the Ovens River catchment. Thus, it seems beneficial taking into account this exhaustive secondary variable (elevation in this study) into the enhanced estimation and mapping of rainfall in both the catchments. Goovaerts (1997) mentioned that use of multiple elevation data other than the colocated positions of rain-gauges can lead to unstable cokriging systems because the correlation between near elevation data is much greater than the correlation between distant rainfall data. Therefore, the colocated elevation data are used for the OCK analysis in this study, which are extracted at the same positions of rain-gauge stations from the DEM of the catchments.

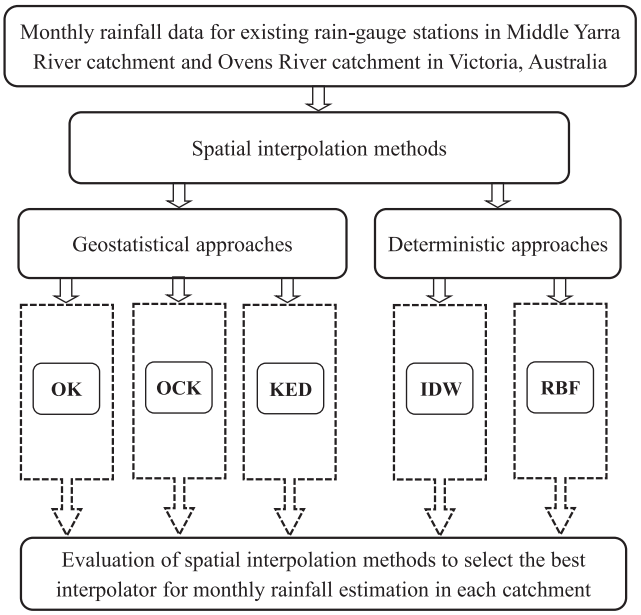

FIGURE 2 Methodological framework adopted in this study. IDW = inverse distance weighting; KED = kriging with an external drift; OCK = ordinary cokriging; OK = ordinary kriging; RBF = radial basis function

3 | METHODOLOGY

The methodological framework adopted in this study for spatial interpolation of rainfall includes three kriging-based geostatistical (OK, OCK, and KED) and two deterministic (IDW and RBF) interpolation methods, which is shown in Figure 2. A brief description of these methods is presented in this section. The variogram and its estimation technique are also summarised with each of the kriging methods because it is a key component of kriging. For a more detailed description of the methods used in the current study, readers are referred to several recent geostatistical textbooks including Journel and Huijbregts (1978); Isaaks and Srivastava (1989), Goovaerts (1997), Chilès and Delfiner (1999), Wackernagel (2003), and Webster and Oliver (2007).

3.1 | Ordinary kriging

Kriging refers to a family of generalized least-squares regression methods in geostatistics that estimate values at unsampled locations using the sampled observations in a specified search neighborhood (Goovaerts, 1997; Isaaks & Srivastava, 1989). OK is a geostatistical interpolation method based on spatially dependent variance, which gives unbiased estimates of variable values at target location in space using the known sampling values at surrounding locations. The unbiasedness in the OK estimates is ensured by forcing the kriging weights to sum to 1. Thus, the OK estimator may be stated as a linear combination of variable values, which is given by

$$\widehat{Z}_{OK}(s_0) = \sum_{i=1}^{n} \omega_i^{OK} Z(s_i) \qquad \text{with} \quad \sum_{i=1}^{n} \omega_i^{OK} = 1 \tag{1}$$

where $\widehat{Z}_{OK}(s_0)$ is the estimated value of variable Z (i.e., rainfall) at target (at which estimation is to be made) unsampled location s_0; ω_i^{OK} indicates the OK weights linked with the sampled location s_i with respect to s_0; and n is the number of sampling points used in estimation. While giving the estimation at target location, OK provides a variance measure to signify the reliability of the estimation.

OK is known as the best linear unbiased estimator (Isaaks & Srivastava, 1989). It is linear in the sense that it gives the estimation based on the weighted linear combinations of observed values. It is best in the sense that the estimate variance is minimized while interpolating the unknown value at desired location. And it is unbiased because it tries to have the expected value of the residual to be zero (Adhikary et al., 2016b). The weight constraint in Equation 1 ensures the unbiased estimation in OK. For OK, the kriging weights are determined to minimize the estimation variance and ensure the unbiasedness of the estimator.

The OK weights ω_i^{OK} can be obtained by solving a system of $(n + 1)$ simultaneous linear equations as follows:

$$\begin{aligned} &\sum_{i=1}^{n} \gamma(s_i - s_j)\omega_i^{OK} + \mu_1^{OK} = \gamma(s_j - s_0) \qquad \text{for } j = 1, \ldots\ldots\ldots, n \\ &\sum_{i=1}^{n} \omega_i^{OK} = 1 \end{aligned} \tag{2}$$

where $\gamma(s_i - s_j)$ is the variogram values between sampling locations s_i and s_j, $\gamma(s_j - s_0)$ is the variogram values between sampling location s_j and the target location, s_0, and μ_1^{OK} is the Lagrange multiplier parameter. Equation 2 indicates that OK highly depends on a mathematical

function called variogram model that indicates the degree of spatial autocorrelation in datasets.

For OK interpolation of variables, first an experimental variogram $\hat{\gamma}(d)$ is derived by

$$\hat{\gamma}(d) = \frac{1}{2N(d)} \sum_{i=1}^{N(d)} [Z(s_i + d) - Z(s_i)]^2 \quad (3)$$

where $Z(s_i)$ and $Z(s_i + d)$ are the variable values at corresponding sampling locations s_i and $(s_i + d)$, respectively, located at d distance apart and $N(d)$ is the number of data pairs. A variogram cloud is initially generated using Equation 3 for observations at any two data points, in which all semivariance values are plotted against their separation distance. The experimental variogram is computed from the variogram cloud by subdividing it into a number of lags and taking an average of each lag interval (Johnston, VerHoef, Krivoruchko, & Lucas, 2001; Robertson, 2008). A variogram model $\gamma(d)$ is then fitted to the experimental variogram. A typical variogram cloud based on Equation 3 and a typical experimental variogram with a typical fitted model is shown in Figure 3.

Exponential, Gaussian, and spherical are the most commonly used variogram models for kriging applications in hydrology (Adhikary et al., 2015), which are also used to model the experimental variogram. The functional forms these variogram models are given in Table 2. The three models are fitted to the experimental variogram using regression by noting the residual sum of squares (RSS) between the experimental $\hat{\gamma}(d_k)$ and modelled $\gamma(d_k)$ variogram values (Mair & Fares, 2011) with a trial-and-error approach for different lag sizes and lag intervals (Goovaerts, 1997) such that the RSS is minimum. RSS is given by

$$\text{RSS} = \sum_{k=1}^{K} [\hat{\gamma}(d_k) - \gamma(d_k)]^2 \quad (4)$$

RSS in Equation 4 provides an exact measure of how well the variogram model fits the experimental variogram (Robertson, 2008). Lag sizes and number of lags are varied based on a general rule of thumb, in which the lag size times the number of lags should be about half of the largest distance among all data pairs in the variogram cloud (Johnston et al., 2001, p. 66). The variogram parameters (nugget, sill, and range) are also iteratively changed to obtain the best fitted model. The model with its corresponding parameters that minimizes RSS is selected as the best variogram model and finally used in OK analysis. Variogram model fitting is performed using GS+ geostatistical software (Robertson, 2008) and OK is implemented through ArcGISv9.3.1 software (ESRI, 2009) and its geostatistical analyst extension (Johnston et al., 2001).

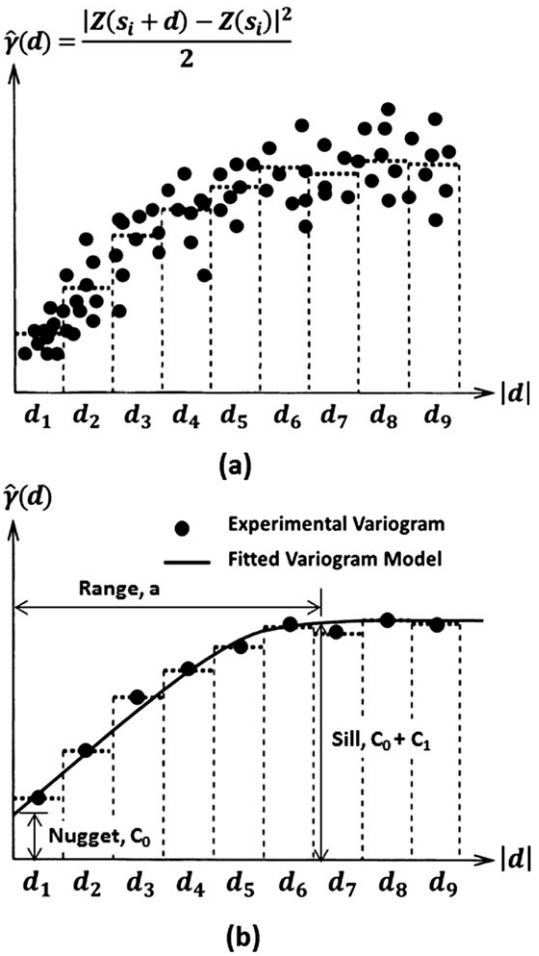

FIGURE 3 (a) a typical variogram cloud for a finite set of discrete lags, and (b) a typical experimental variogram based on the variogram cloud fitted by a typical variogram model with its parameters

3.2 | Ordinary cokriging

OCK method is a modification of the OK method. The key advantage of OCK is that it can make use of more than one variable rather than using only a single variable in the estimation process. The OCK method is used to enhance the estimation of primary variable by using secondary variable assuming that the variables are correlated to each other (Isaaks & Srivastava, 1989). In this study, rainfall and elevation are considered, respectively, as the primary and secondary variables in the OCK method. Like OK method, the aim of the OCK method is to estimate the primary variable. The OCK estimator (Goovaerts, 1997) considering one secondary variable (i.e., elevation), which is cross-correlated with the primary variable (i.e., rainfall) may be written as

$$\hat{Z}_{OCK}(s_0) = \sum_{i_1=1}^{n} \omega_{i_1}^{OCK} Z(s_{i_1}) + \sum_{i_2=1}^{m} \omega_{i_2}^{OCK} V(s_{i_2}) \quad (5)$$

$$\text{with} \quad \sum_{i_1=1}^{n} \omega_{i_1}^{OCK} = 1; \sum_{i_2=1}^{m} \omega_{i_2}^{OCK} = 0$$

where $\hat{Z}_{OCK}(s_0)$ is the estimated value of primary variable at target unsampled location s_0, $\omega_{i_1}^{OCK}$ and $\omega_{i_2}^{OCK}$ are the kriging weights associated with the sampling locations of the primary and secondary variables Z

TABLE 2 Commonly used positive-definite variogram models

Model name	Model equation
Exponential	$\gamma(d) = C_0 + C_1\left[1 - \exp\left(-\frac{3d}{a}\right)\right]$
Gaussian	$\gamma(d) = C_0 + C_1\left[1 - \exp\left(-\frac{3d^2}{a^2}\right)\right]$
Spherical	$\gamma(d) = C_0 + C_1\left[\frac{3}{2}\left(\frac{d}{a}\right) - \frac{1}{2}\left(\frac{d^3}{a^3}\right)\right]$, $d<a$ $= C_0 + C_1$, $d \geq a$

C_0 = nugget coefficient, $C_0 + C_1$ = Sill, a = range of variogram model. d = distance of separation between two locations.

and *V*, respectively, *n* and *m* are the number of sampling points for the primary and secondary variables.

The OCK weights are obtained by solving a system of (*n* + 2) simultaneous linear equations (Goovaerts, 1997) that can be given by

$$\begin{aligned}
&\sum_{i_1=1}^{n}\gamma_{zz}\left(s_{i_1}-s_{j_1}\right)\omega_{i_1}^{OCK}+\sum_{i_2=1}^{m}\gamma_{zv}\left(s_{i_2}-s_{j_1}\right)\omega_{i_2}^{OCK}+\mu_1^{OCK}=\gamma_{zz}\left(s_{j_1}-s_0\right) \quad for\ j_1=1,\ldots\ldots,n\\
&\sum_{i_1=1}^{n}\gamma_{vz}\left(s_{i_1}-s_{j_2}\right)\omega_{i_1}^{OCK}+\sum_{i_2=1}^{m}\gamma_{vv}\left(s_{i_2}-s_{j_2}\right)\omega_{i_2}^{OCK}+\mu_2^{OCK}=\gamma_{vz}\left(s_{j_2}-s_0\right) \quad for\ j_2=1,\ldots\ldots,m\\
&\sum_{i_1=1}^{n}\omega_{i_1}^{OCK}=1\\
&\sum_{i_2=1}^{m}\omega_{i_2}^{OCK}=0
\end{aligned} \tag{6}$$

where $\gamma_{zv}\left(s_{i_2}-s_{j_1}\right)$ and $\gamma_{vz}\left(s_{i_1}-s_{j_2}\right)$ are the cross-variogram values between sampled Z and V values, and μ_1^{OCK} and μ_2^{OCK} are the Lagrange multiplier parameters accounting for the two unbiased conditions.

The elementary step in the OCK method is to establish an appropriate model for cross continuity and dependency between the primary (rainfall) and secondary (elevation) variable. This positive correlation between variables is referred to as the cross-regionalization or coregionalization (Goovaerts, 1997; Wackernagel, 2003), which can be quantified by cross-variogram or cross-covariance. These models are used to define the cross continuity and dependency between two variables in the OCK method (Subyani & Al-Dakheel, 2009). The cross-variogram models between the primary (rainfall) and secondary (elevation) variables in the OCK method are obtained by fitting with an experimental cross-variogram that is given by

$$\widehat{\gamma}_{zv}=\widehat{\gamma}_{vz}=\frac{1}{2N(d)}\sum_{i=1}^{N(d)}\left[Z(s_i+d)-Z(s_i)\right]\times\left[V(s_i+d)-V(s_i)\right] \tag{7}$$

It is important to note that the variogram models must satisfy the positive-definite condition (PDC) in kriging. For a single variable (rainfall) in the OK method, the condition is satisfied by using the positive-definite variogram model functions given in Table 2. However, the OCK method considering two variables (rainfall and elevation) consists of one cross-variogram and two direct variograms, and additional requirement for satisfying the PDC (Goovaerts, 1999). In order to make sure that the cross-variogram model is positive-definite (all eigenvalues are positive), an indicator called the Cauchy-Schwarz inequality (Journel & Huijbregts, 1978; Phillips et al., 1992) must be satisfied for all distance values *d*, which is given by

$$\gamma_{zv}(d)\le\left[\gamma_{zz}(d)\gamma_{vv}(d)\right]^{\frac{1}{2}} \tag{8}$$

where $\gamma_{zv}(d)$ is the cross-variogram model between primary and secondary variables, and $\gamma_{zz}(d)$ and $\gamma_{vv}(d)$ are the direct variogram models for primary and secondary variables, respectively. Based on the indicator shown in Equation 8, Hevesi et al. (1992) suggested a graphical test of PDC for the fitted models as follows:

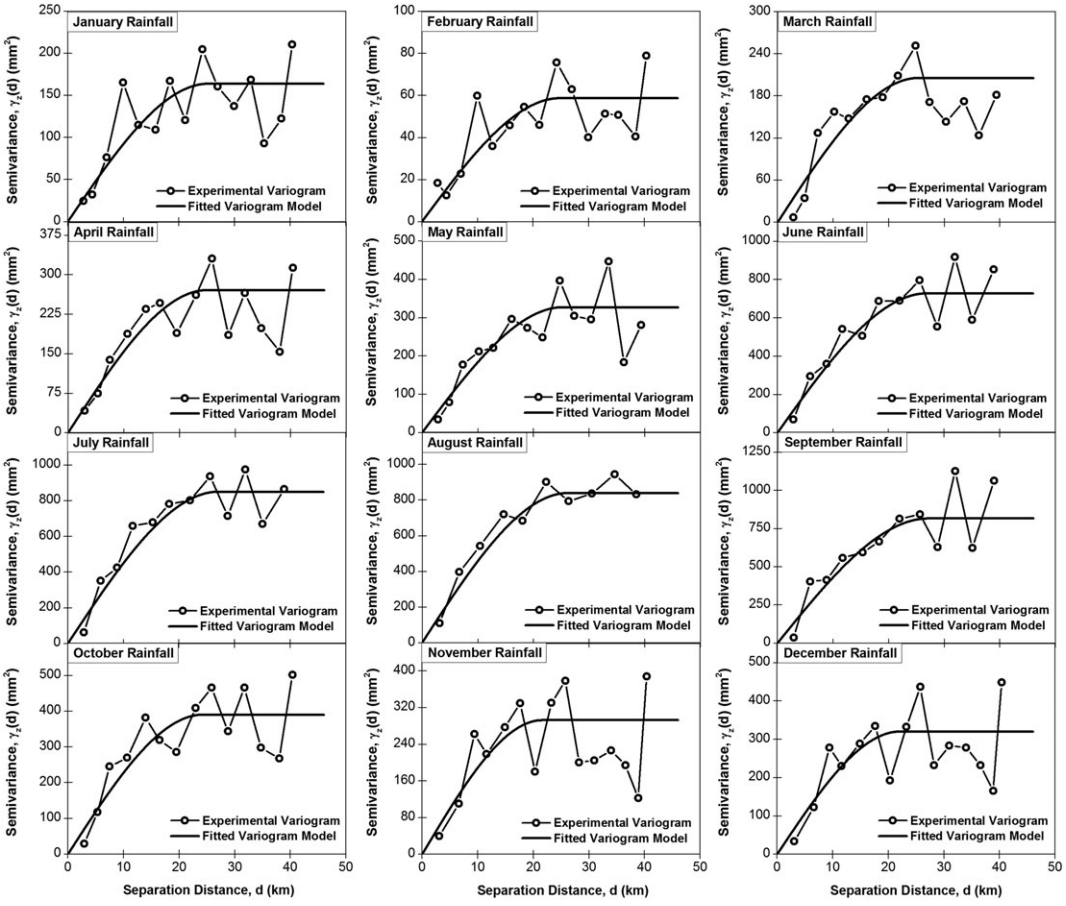

FIGURE 4 Experimental variograms and fitted variogram models for the monthly rainfall data of the Middle Yarra River catchment used in the ordinary kriging interpolation method

$$\mathrm{PDC} = [\gamma_{zz}(d)\gamma_{vv}(d)]^{\frac{1}{2}} \quad (9)$$

The model is considered positive-definite if the absolute value of the cross-variogram model $\gamma_{zv}(d)$ in Equation 8 is less than the slope and corresponding absolute value of PDC curve in Equation 9 for all distance values d. In the OCK method, direct and cross-variogram models are fitted as linear combination of the same set of basic models given in Table 2 such that the RSS value by Equation 4 is minimum under the requirement of PDC. Variogram model fitting is performed using GS+ geostatistical software (Robertson, 2008) and OCK is implemented through ArcGISv9.3.1 software (ESRI, 2009) and its geostatistical analyst extension (Johnston et al., 2001).

3.3 | Kriging with an external drift

KED is a particular type of universal kriging that gives the estimation of a primary variable Z, known only at a small number of locations in the study catchment, through a secondary variable V, exhaustively known in the same area (Feki et al., 2012). The trend or local mean of the primary variable is first derived using the secondary variable (Goovaerts, 1997; Wackernagel, 2003) and then simple kriging is carried out on residuals from the local mean. The KED estimator (Wackernagel, 2003) is generally given as

$$\widehat{Z}_{KED}(s_0) = \sum_{i=1}^{n} \omega_i^{KED} Z(s_i) \quad \text{with} \quad \sum_{i=1}^{n} \omega_i^{KED} = 1 \quad (10)$$

The KED weights ω_i^{KED} can be obtained by solving a system of $(n + 2)$ simultaneous linear equations as follows:

$$\begin{aligned} &\sum_{i=1}^{n} \gamma_R(s_i - s_j)\omega_i^{KED} + \mu_0^{KED} + \mu_1^{KED} V(s_j) = \gamma_R(s_j - s_0) \quad \text{for } j = 1, \ldots, n \\ &\sum_{i=1}^{n} \omega_i^{KED} = 1 \\ &\sum_{i=1}^{n} \omega_i^{KED} V(s_i) = V(s_0) \end{aligned} \quad (11)$$

where $\gamma_R(s_i - s_j)$ is the residual variogram values between sampling locations s_i and s_j, $\gamma_R(s_j - s_0)$ is the residual variogram values between sampling location s_j and the target location, s_0, and μ_0^{KED} and μ_1^{KED} are the Lagrange multiplier parameters.

OCK and KED differ in the way the secondary variable V is used. The secondary variable (e.g., elevation in this study) gives only the trend information in KED, whereas estimation with OCK is directly influenced by it (Delbari et al., 2013). In case of KED, the primary and secondary variables should exhibit a linear relationship. In addition, estimation with KED requires the secondary variable values at all the

TABLE 3 Results of fitted variogram models for monthly rainfall data for using in the OK interpolation method

		Variogram parameters			Cross-validation statistics	
Month	Model name	Nugget, C_0 (mm^2)	Sill, $C_0 + C_1$ (mm^2)	Range, a (km)	SM	SRMS
Middle Yarra River catchment						
January	Spherical	0.15	163.65	25.20	0.068	0.998
February	Spherical	0.20	58.70	24.75	0.059	1.000
March	Spherical	0.00	205.38	25.25	0.059	0.863
April	Spherical	1.25	270.75	24.85	0.054	0.897
May	Spherical	1.10	327.20	25.25	0.039	0.916
June	Spherical	0.10	727.60	26.85	0.041	0.847
July	Spherical	0.10	849.60	27.00	0.031	0.795
August	Spherical	4.00	839.00	26.11	0.035	0.851
September	Spherical	1.00	816.00	27.07	0.045	0.883
October	Spherical	0.00	390.00	24.18	0.049	0.903
November	Spherical	0.00	292.50	21.53	0.058	0.861
December	Spherical	0.00	320.00	22.00	0.060	0.863
Ovens River catchment						
January	Spherical	92.00	455.00	109.50	-0.048	0.992
February	Spherical	83.00	360.00	70.00	0.007	1.024
March	Spherical	85.00	501.00	107.10	-0.021	0.991
April	Gaussian	93.00	793.00	162.29	-0.060	1.000
May	Spherical	109.00	1016.00	108.60	-0.047	1.016
June	Spherical	50.00	1240.00	90.00	-0.039	1.001
July	Gaussian	180.00	2030.00	80.50	-0.083	0.992
August	Spherical	58.00	1420.00	65.00	-0.040	0.990
September	Spherical	25.00	937.00	67.00	-0.028	0.997
October	Spherical	102.00	519.00	75.40	-0.027	1.001
November	Spherical	19.00	430.00	68.00	0.001	0.988
December	Spherical	35.00	296.00	89.10	-0.028	0.988

Note. OK = ordinary kriging; SM = standardized mean error; SRMS = standardized root mean square error.

estimation grid nodes as well as all the sampling locations s_i. The residual variogram models are fitted based on the basic models in Table 2 such that the RSS value between the experimental and modelled variogram values by Equation 4 is minimum. Variogram model fitting and estimation with KED are performed using GS+ geostatistical software (Robertson, 2008).

3.4 | Inverse distance weighting

IDW interpolation method (ASCE, 1996) gives a linear weighted average of several neighbouring observations to estimate the variable value at target location. This method assumes that each observation point has local influence that diminishes with distance. IDW assigns greater weights to observation points near to the target location, and the weights diminish as a function of distance (Johnston et al., 2001). The estimation by IDW can be written as

$$\widehat{Z}(s_0) = \sum_{i=1}^{n} \omega_i Z(s_i) \qquad where \quad \omega_i = d_{i0}^{-k} / \sum_{i=1}^{n} d_{i0}^{-k} \tag{12}$$

where $\widehat{Z}(s_0)$ is the estimated rainfall value at desired location s_0, $Z(s_i)$ is the Z value at location s_i, ω_i is the weight assigned to observation points, d_{i0} is the distance between the sampling point at locations s_i and s_0, n is the number of sampling points, and k is a power, which is referred to as a control parameter.

As "k" approaches zero and the weights becomes more similar, IDW estimates approach the simple average of the surrounding observations. However, the effect of the farthest observations on the estimated value is diminished with the increase of k. The value of k ranges from 1 to 6 (Teegavarapu & Chandramouli, 2005). Several studies have investigated with variations in a power to examine its effects on the spatial distribution of information from rainfall observations (Chen & Liu, 2012). Therefore, k value is varied in the range of 1 to 6 with an increment of 0.1 in the current study. The optimal k value is selected based on the lowest RMSE value between the observed and estimated values. All rain-gauge stations are considered in the search neighbourhood in the estimation process. IDW interpolation is performed by ArcGISv9.3.1 software (ESRI, 2009) and its geostatistical analyst extension (Johnston et al., 2001).

3.5 | Radial basis function

RBF (Chilès & Delfiner, 1999) is an exact interpolation method, which stands for a diverse group of interpolation methods. The RBF estimator can be viewed as a weighted linear function of distance from grid point to data point plus a bias factor, which is given by

$$\widehat{Z}(s_0) = \sum_{i=1}^{n} \omega_i \varnothing(\|s_i - s_0\|) + \mu \tag{13}$$

where $\varnothing(r)$ is the radial basis function ($r = \|s_i - s_0\|$), r is the radial distance from target point s_0 to sampling points s_i, ω_i are the weights and μ is the Lagrangian multiplier. The weights are obtained by solving of a system of (n + 1) simultaneous linear equations.

The basis kernel functions in the RBF method are analogous to variograms in kriging, which makes it similar to geostatistical interpolation methods. However, RBF does not have the advantage of a prior analysis of spatial correlation unlike kriging. When interpolating a grid node, the basis kernel functions define the optimal set of weights to be used with the sampling points. There are several radial basis functions available (Johnston et al., 2001) However, thin plate spline is the most commonly used radial basis function for interpolation (e.g., Boer, de Beurs, & Hartkamp, 2001; Di Piazza et al., 2011; Hutchinson, 1995). In this study, thin plate spline is also used as the radial basis function, which is given by

$$\varnothing(r) = (cr)^2 \ln(cr) \tag{14}$$

where c is the smoothing parameter, which is obtained through cross-validation process. The optimal value of the smoothing parameter is selected based on the lowest RMSE value between the observed and estimated values. RBF interpolation method is performed by ArcGISv9.3.1 software (ESRI, 2009) and its geostatistical analyst extension (Johnston et al., 2001).

3.6 | Assessment of interpolation methods

The performance of different interpolation methods (OK, OCK, KED, IDW, and RBF) used in this study are evaluated and compared through cross-validation process. The cross-validation is a simple leave-one-out

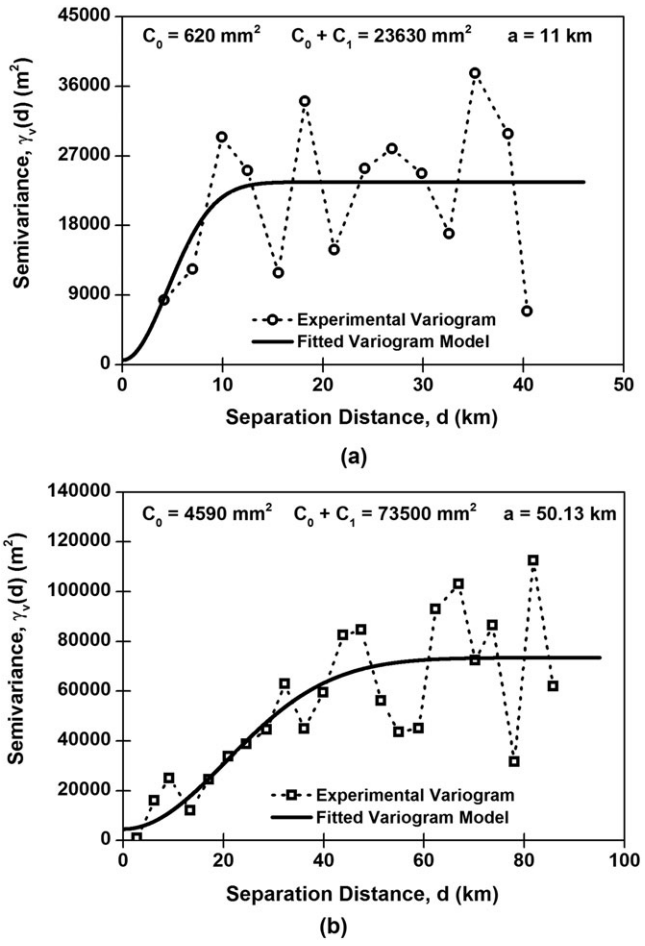

FIGURE 5 Experimental variograms and fitted variogram models based on the collocated elevation data for (a) Middle Yarra River catchment, and (b) Ovens River catchment

validation procedure (Haddad, Rahman, Zaman, & Shrestha, 2013) in which observations are removed one at a time from the dataset and then re-estimated from the remaining observations using the adopted model. Cross-validation provides important evidence of the performance measures for the interpolation methods. In this study, the performance of all the interpolation methods for rainfall estimation is compared based on mean bias error (MBE), RMSE, and coefficient of determination (R^2) values between the observed and estimated rainfall values, which are given by Equations 15–17.

$$\text{MBE} = \frac{1}{n}\sum_{i=1}^{n}\left[Z(s_i)-\widehat{Z}(s_i)\right] \tag{15}$$

$$\text{RMSE} = \sqrt{\frac{1}{n}\sum_{i=1}^{n}\left[Z(s_i)-\widehat{Z}(s_i)\right]^2} \tag{16}$$

$$R^2 = \frac{\left[\sum_{i=1}^{n}\{Z(s_i)-Z_m\}\left\{\widehat{Z}(s_i)-\widehat{Z}_m\right\}\right]^2}{\sum_{i=1}^{n}\{Z(s_i)-Z_m\}^2\sum_{i=1}^{n}\left\{\widehat{Z}(s_i)-\widehat{Z}_m\right\}^2} \tag{17}$$

In Equations 15–17, $Z(s_i)$ and $\widehat{Z}(s_i)$ are the observed and predicted values, Z_m and $\widehat{Z}_m$ are the mean of the observed and predicted values, and n is the number of sampled data points. The interpolation method with the lowest MBE and RMSE values and the highest R^2 value is chosen as the best interpolation method.

As has been mentioned earlier, kriging gives the prediction standard error while giving the estimation of unsampled variables, the adequacy of the variogram model for kriging and cokriging estimation should also be tested to produce correct interpolation results (Johnston et al., 2001; Phillips et al., 1992). Therefore, two additional standardized cross-validation statistics are used in this study, which are standardized mean error (SM) and standardized root mean square error (SRMS) as given by Equations 18–19

$$\text{SM} = \frac{1}{n}\sum_{i=1}^{n}\frac{\left[Z(s_i)-\widehat{Z}(s_i)\right]}{\widehat{\sigma}(s_i)} \tag{18}$$

$$\text{SRMS} = \sqrt{\frac{1}{n}\sum_{i=1}^{n}\left[\frac{Z(s_i)-\widehat{Z}(s_i)}{\widehat{\sigma}(s_i)}\right]^2} \tag{19}$$

where $\widehat{\sigma}(s_i)$ is the prediction standard error for location s_i. SM should be close to 0 if the estimates using the adopted variogram model are unbiased. SRMS should be close to 1 if the estimation variances are consistent and the variability of the prediction is correctly assessed (Adhikary et al., 2015; Johnston et al., 2001).

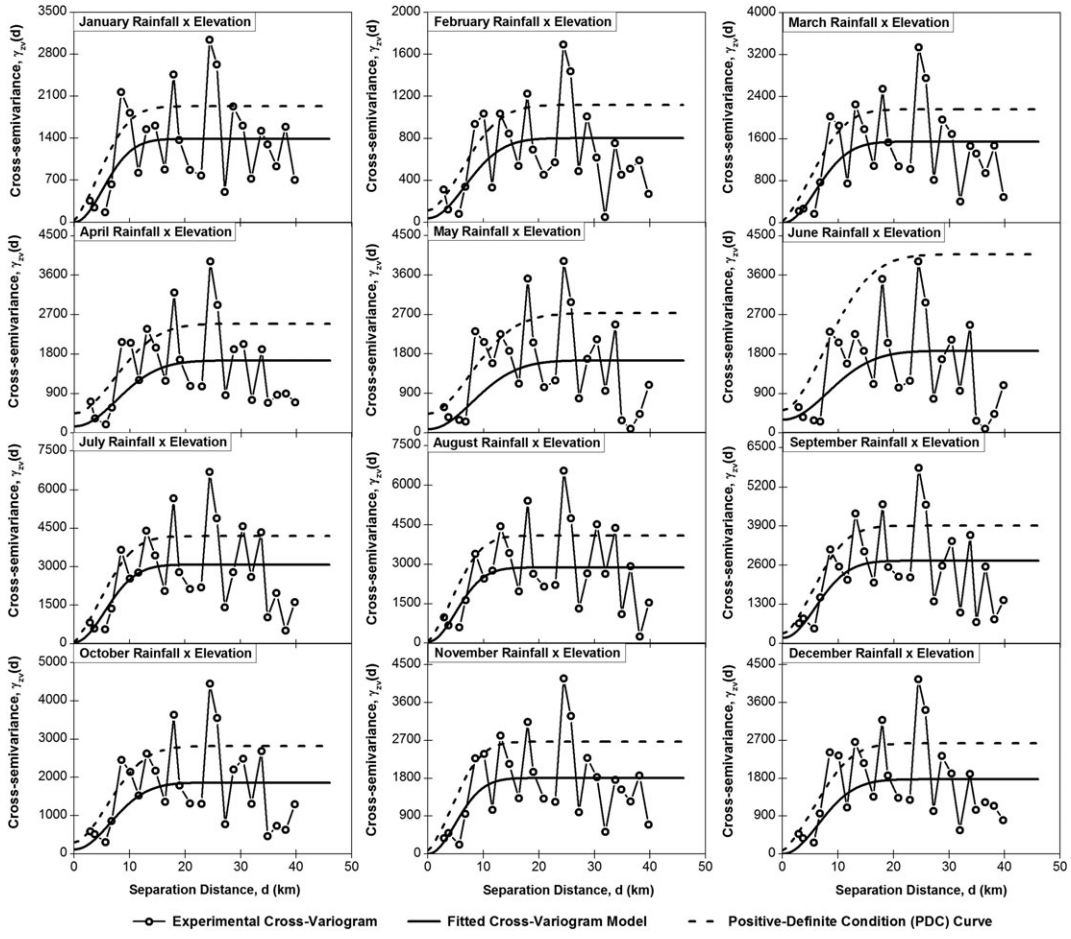

FIGURE 6 Experimental cross-variograms with the fitted cross-variogram models and positive-definite condition curve based on the monthly rainfall and collocated elevation data for the Middle Yarra River catchment used in the ordinary cokriging interpolation method

4 | RESULTS AND DISCUSSION

4.1 | Variogram models for OK analysis

The OK analysis requires the estimation of the direct variogram models for rainfall data. In this study, an isotropic experimental variogram is estimated from the rainfall dataset for each month assuming an identical spatial correlation in all directions and neglecting the influence of anisotropy on the variogram parameters. Isotropy is assumed for the methodological simplicity. Isotropy is a property of a natural process or data where directional influence is considered insignificant and spatial dependence (autocorrelation) changes only with the distance between two locations (Johnston et al., 2001). Under the isotropic condition, the semivariance is assumed the same for a given distance, regardless of direction. Initially, the directional experimental variograms are estimated from each monthly rainfall dataset. However, the directional variograms are found noisy because of the less number of rain-gauge stations in the study area. Therefore, the directional influence is ignored in the experimental variogram calculation. The experimental variogram is then fitted with three predefined variogram model functions (exponential, Gaussian, and spherical as given in Table 2) to obtain the variogram models for each monthly rainfall dataset.

For convenience in this study, results obtained for the Middle Yarra River catchment are presented and discussed elaborately and compared with that obtained for the Ovens River catchment. Figure 4 shows the experimental variograms and fitted variogram models with optimal variogram parameters (i.e., nugget, sill, and range) for monthly rainfall data of the Middle Yarra River catchment, which are used in OK analysis. The best fitted variogram models are selected based on the minimum RSS values using a trial-and-error process with different lag intervals. The variogram parameters are iteratively changed to get the best fitted model, which yields the minimum RSS. As can be seen from Figure 4, the spherical model is the best fitted variogram model for all months having spatial structure of $.66 < R < .97$ (results of R not shown in Figure). It can be also noted that 10 months (except November and December) have R values greater than .75. The optimal variogram parameters for each monthly rainfall dataset for both the catchments are provided in Table 3. As can be seen from Table 3, the ratio of nugget coefficient to sill of the variogram model is small for all months for both the catchments. This evidently indicates that a strong spatial correlation exists between the monthly mean rainfall and the spatial distribution of the rain-gauge stations over the study area. This supports the use of geostatistical interpolation methods such as OK, OCK, and KED, which consider

TABLE 4 Results of fitted cross-variogram models between monthly rainfall and elevation for using in the OCK interpolation method

		Variogram parameters			Cross-validation statistics	
Month	Model name	Nugget, C_0 (mm^2)	Sill, $C_0 + C_1$ (mm^2)	Range, a (km)	SM	SRMS
Middle Yarra River catchment						
January	Gaussian	1.0	1387.0	12.65	0.053	1.001
February	Gaussian	40.0	801.0	16.19	0.067	1.000
March	Gaussian	1.0	1545.0	14.36	0.055	1.006
April	Gaussian	150.0	1653.0	18.35	0.057	1.004
May	Gaussian	80.0	1651.0	19.40	0.042	1.019
June	Gaussian	300.0	1874.5	19.75	0.055	1.001
July	Gaussian	55.0	3081.2	13.50	0.008	1.002
August	Gaussian	57.5	2872.9	12.10	0.007	1.006
September	Gaussian	179.4	2746.0	14.25	0.042	1.002
October	Gaussian	114.5	1860.9	15.85	0.053	1.004
November	Gaussian	3.4	1804.4	12.00	0.034	1.000
December	Gaussian	1.7	1774.7	15.66	0.096	1.002
Ovens River catchment						
January	Gaussian	485.2	2197.9	60.98	-0.020	0.989
February	Gaussian	525.8	2540.3	50.56	0.001	1.119
March	Gaussian	635.1	2349.5	52.45	-0.012	1.093
April	Gaussian	373.7	2209.3	36.01	-0.019	0.904
May	Gaussian	595.0	3170.7	32.99	-0.015	1.090
June	Gaussian	342.6	3961.7	52.48	-0.022	1.117
July	Gaussian	652.2	4175.6	71.62	-0.030	1.028
August	Gaussian	919.2	4223.1	96.48	-0.024	1.095
September	Gaussian	733.6	3717.8	66.49	-0.018	1.000
October	Gaussian	256.0	2048.1	29.73	-0.010	1.010
November	Gaussian	413.5	1925.5	64.09	-0.013	1.050
December	Gaussian	123.5	1935.7	32.60	-0.021	1.007

Note. OCK = ordinary cokriging; SM = standardized mean error; SRMS = standardized root mean square error.

the spatial correlation in the estimation process. The range of influence and the sill of the variogram model vary from one month to another, but the variogram exhibit a same spherical structure in all months. This may be caused due to the control of the relief on the spatial distribution of rainfall (Delbari et al., 2013). The range of influence is lowest for November (21.53 km) and highest for September (27.07 km). Furthermore, the cross-validation statistics in Table 3 for both the catchments confirm that the fitted variogram models for all monthly rainfall data satisfy the unbiased condition and thus can be used for the OK analysis.

For elevation data, an isotropic experimental variogram is computed ignoring the directional influence. The experimental variogram is then fitted with the aforementioned three variogram model functions. The best fitted variogram model is selected using the same procedure described above. The Gaussian variogram model gives the best fitted model for both the catchments with the lowest RSS value, which is shown in Figure 5. The optimal variogram parameters for both the catchments are also shown in the figure. In order to avoid possible inconsistencies in the subsequent modelling of direct and cross-variograms in OCK analysis (Goovaerts, 1997, 2000), the colocated elevation data (see Figure 1) are used for estimating the variogram of elevation, not the entire DEM of the catchment. Therefore, the cokriging method adopted in this study is referred to as the colocated OCK method (Wackernagel, 2003).

4.2 | Cross-variogram models for OCK analysis

The OCK analysis requires the simultaneous estimation of the direct and cross-variogram models for the rainfall and elevation variables. The three variogram models are fitted as a linear combination of the same set of standard models given in Table 2 so that the RSS value is minimum under the constraints of PDC (Goovaerts, 1999). Figure 6 shows the experimental and fitted cross-variogram models for the Middle Yarra River catchment. The number of data pairs in each lag size is the same for all the three direct and cross-variogram models. Figure 6 also shows the PDC curve computed based on Equation 9 to examine the positive-definiteness criteria of the cross-variogram models obtained for the catchment. Additionally, the cross-validation statistics are used for identifying the adequacy and final selection of the adopted cross-variogram model for the OCK analysis. The cross-validation results obtained using all the adopted cross-variogram models for both the catchments are presented in Table 4. The results in Table 4 indicate that the cross-variogram models of all monthly datasets are suitable for the OCK analysis considering all neighbourhoods for both the catchments.

As can be seen from Figure 6, the Gaussian variogram model fits well for all monthly datasets of the Middle Yarra River catchment, which also satisfy the PDC criteria defined by Equation 9. Furthermore, the correlation between monthly rainfall and elevation for all

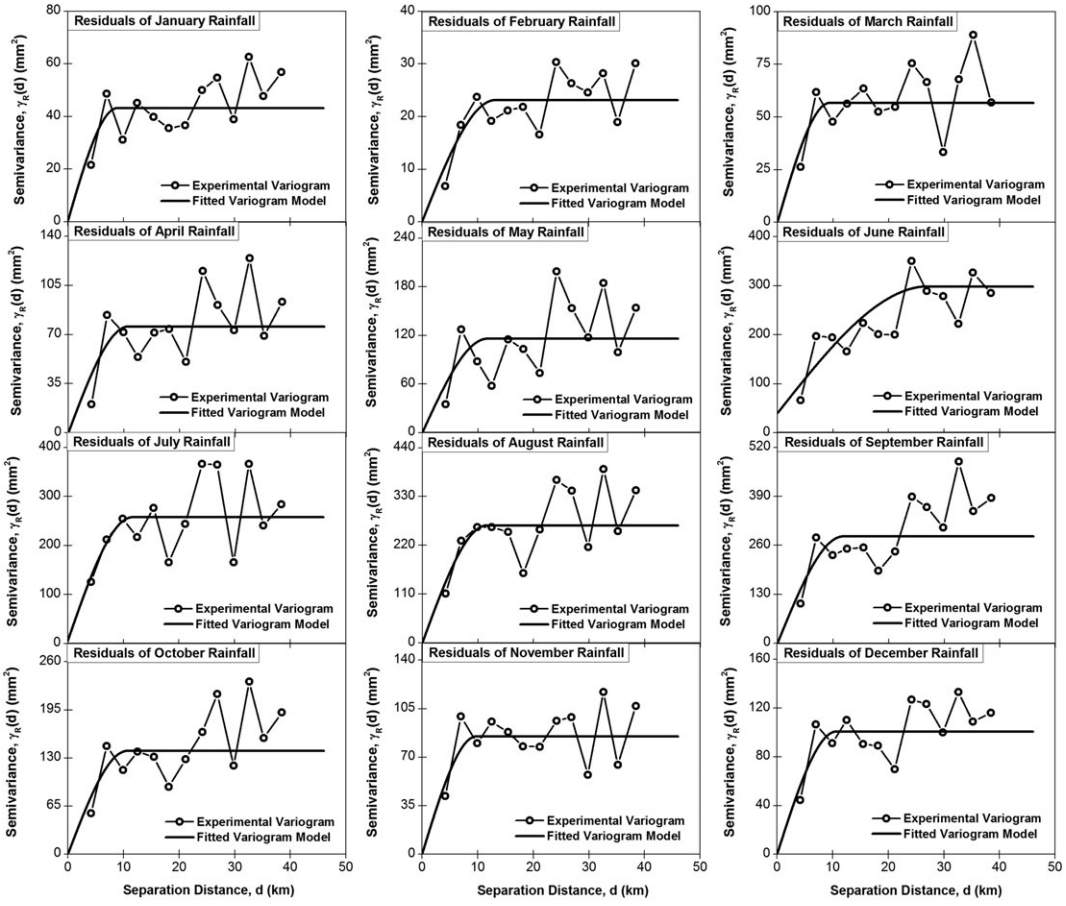

FIGURE 7 Experimental residual variograms and fitted residual variogram models for the Middle Yarra River catchment used in the kriging with an external drift interpolation method

months in Table 1 indicates that elevation will contribute to enhance the monthly rainfall estimation in the catchment. The figure also shows that the values of the sample cross-variogram increase for distances from 0 to 25 km (more than half of the maximum interstation distance) for almost all months. This indicates that a positive spatial cross-correlation exists between rainfall and elevation in the catchment. This wide ranges may be due to the high correlation (.67 < R < .79) between the monthly rainfall and elevation (Table 1). Such high correlation confirms that the monthly rainfall in the Middle Yarra River catchment is mainly caused by the orographic effects.

Figure 6 also shows the PDC curves, which are computed to examine the positive-definite conditions of the cross-variogram models of the catchment. It is worth pointing out that the PDC curve may give a qualitative indication for the degree of correlation. As can be observed from Figure 6, the plotted PDC curve for most of the months showed a close fit to the cross-variogram model for smaller distances with few exceptions (February, April, May, and June months). For example, the PDC curve is closer to the cross-variogram model in the case of January, March, July, November, and December months depending on the degree of correlation. This conclusion holds true based on the higher correlation for these months as given in Table 1.

4.3 | Residual variogram models for KED analysis

In order to implement the KED analysis, experimental residual variograms are estimated based on the residuals obtained from linear regression between rainfall and elevation data neglecting the influence of anisotropy on the variogram parameters. The experimental residual variogram is then fitted using the three standard models given in Table 2. Figure 7 shows the experimental and fitted residual variogram models for all monthly datasets of the Middle Yarra River catchment. It can be seen from the figure that the spherical model gives the best fitted model for all monthly datasets. The optimal variogram parameters and the corresponding cross-validation statistics of the selected residual variogram models for both the catchments are presented in Table 5. As can be also seen from Figure 7 and Table 5, the residual variogram models exhibit relatively smaller sills than those obtained from the actual rainfall datasets (see Figure 4) but they follow very similar structure. This is not unexpected because the residual variograms from the linear regression represents variation, which remains after removing the trend (Lloyd, 2005). The cross-validation statistics shown in Table 5 also indicate that the residual variogram models of all monthly datasets for both the catchments are satisfactory for the KED analysis.

TABLE 5 Results of fitted residual variogram models for using in the KED interpolation method

		Variogram parameters			Cross-validation statistics	
Month	Model name	Nugget, C_0 (mm^2)	Sill, $C_0 + C_1$ (mm^2)	Range, a (km)	SM	SRMS
Middle Yarra River catchment						
January	Spherical	0.10	43.14	8.86	0.029	1.022
February	Spherical	0.01	23.11	13.10	0.025	0.981
March	Spherical	0.10	56.69	9.35	0.060	0.999
April	Spherical	0.10	75.70	10.76	0.010	1.000
May	Spherical	0.10	115.80	11.61	-0.034	1.031
June	Spherical	39.90	298.70	27.03	0.005	0.981
July	Spherical	5.70	257.70	11.59	-0.024	0.990
August	Spherical	0.10	265.00	11.57	-0.013	0.984
September	Spherical	0.10	283.50	11.77	0.027	0.982
October	Spherical	0.10	139.40	10.60	-0.010	1.004
November	Spherical	0.10	84.94	9.69	0.054	0.992
December	Spherical	0.10	100.70	10.61	0.058	0.990
Ovens River catchment						
January	Spherical	38.90	239.40	42.90	-0.017	1.012
February	Spherical	60.10	320.90	32.72	0.004	1.029
March	Spherical	13.40	246.20	26.80	-0.011	0.996
April	Gaussian	67.20	188.00	103.05	-0.043	1.008
May	Spherical	217.00	597.00	108.40	-0.026	1.071
June	Spherical	60.00	841.00	70.20	-0.044	1.028
July	Spherical	5.00	1713.00	106.00	-0.092	1.005
August	Gaussian	250.00	2084.00	90.54	-0.045	1.001
September	Spherical	1.00	975.00	100.85	-0.027	1.029
October	Spherical	42.10	383.60	87.00	-0.018	1.041
November	Spherical	6.00	367.30	92.30	-0.012	0.989
December	Spherical	31.00	192.50	88.75	-0.028	0.993

Note. KED = kriging with an external drift; SM = standardized mean error; SRMS = standardized root mean square error.

4.4 | Spatial prediction of rainfall

In this study, different geostatistical and deterministic interpolation methods including OK, OCK, KED, IDW, and RBF are adopted to estimate the spatial distribution of monthly mean rainfall in the Middle Yarra River catchment and the Ovens River catchment in Australia. Several performance measures including MBE, RMSE, and R^2 are frequently used to indicate how accurately an interpolator predicts the observed data. Smaller values of MBE and RMSE with a higher R^2 value of an interpolator indicate better prediction by the corresponding method. In case of the scatter plot, the better prediction is that if all scattered points lay close to the 45^0 line with the highest R^2 value between the predicted and observed values (Adhikary et al., 2016a).

Table 6 presents the different performance measures of the adopted interpolation methods (or interpolators) for estimating monthly rainfall over both the study catchments. The different interpolation methods are quantitatively compared based on these performance measures in order to identify the best interpolator for each of the catchment. As can be seen from the table, geostatistical (OK, OCK, and KED) interpolation methods perform better than deterministic (IDW and RBF) interpolation methods for monthly rainfall estimation in the study area. The OCK method gives the best results for rainfall estimation over the study area for all months when considering all the performance measures. The KED method gives the second best results, which is very close to the performance of the OCK method but performs better than the OK method for both the catchments. IDW and RBF give similar performance with higher error in rainfall estimation over the study area. For the Middle Yarra River catchment, Table 6 also shows that in some months, the RBF method performs better than the OK method for rainfall estimation. However, no remarkable differences are seen between them when considering all the performance measures.

For OK, OCK, KED, IDW, and RBF methods, the average RMSE values (Table 6) for the Middle Yarra River catchment are 11.93, 10.29, 10.85, 12.66, and 12.22 mm, respectively, whereas the average RMSE values for the Ovens River catchment are 17.42, 16.15, 16.65, 17.54, and 23.41 mm, respectively. For OK, OCK, KED, IDW, and

TABLE 6 Performance of different interpolation (OK, OCK, KED, IDW, and RBF) methods for monthly rainfall estimation in the study area

	MBE (mm)					RMSE (mm)					R^2				
Month	OK	OCK	KED	IDW	RBF	OK	OCK	KED	IDW	RBF	OK	OCK	KED	IDW	RBF
Middle Yarra River catchment															
January	0.98	0.63	0.73	1.76	1.56	8.92	6.96	7.99	8.96	9.99	0.40	0.66	0.56	0.42	0.31
February	0.51	0.38	0.41	0.73	0.85	5.25	3.80	4.45	5.26	5.46	0.42	0.71	0.59	0.42	0.42
March	0.97	0.65	0.70	1.67	1.78	8.71	6.79	8.41	9.58	9.50	0.54	0.73	0.58	0.45	0.46
April	1.03	0.83	0.89	1.70	2.27	9.80	8.26	8.75	10.68	10.04	0.54	0.67	0.64	0.46	0.55
May	0.78	0.72	-0.40	1.43	2.41	11.55	10.78	11.98	11.58	11.80	0.49	0.56	0.51	0.49	0.55
June	1.19	1.26	1.17	2.25	3.29	15.15	13.77	13.44	17.26	15.15	0.61	0.67	0.69	0.49	0.63
July	0.89	0.11	-0.36	1.73	2.77	15.50	14.63	14.84	16.85	15.01	0.65	0.69	0.68	0.59	0.68
August	1.05	0.03	-0.20	2.08	3.04	16.75	15.94	14.67	18.19	16.12	0.59	0.63	0.69	0.52	0.64
September	1.38	0.87	0.92	2.69	3.52	16.79	15.73	15.38	18.46	17.17	0.57	0.62	0.63	0.48	0.57
October	1.07	0.79	-0.11	1.86	2.32	12.34	10.70	11.56	12.05	12.48	0.53	0.64	0.60	0.56	0.56
November	1.23	0.55	0.58	2.16	2.28	11.00	8.25	9.10	11.43	11.72	0.50	0.73	0.66	0.47	0.46
December	1.31	1.07	1.08	2.25	2.28	11.43	7.93	9.58	11.65	12.17	0.51	0.78	0.66	0.50	0.48
Average	1.03	0.66	0.45	1.86	2.36	11.93	10.29	10.85	12.66	12.22	0.53	0.67	0.62	0.49	0.54
Ovens River catchment															
January	-0.62	-0.56	-0.25	-1.78	-1.13	12.86	12.39	12.45	13.68	18.42	0.41	0.44	0.42	0.34	0.18
February	0.11	-0.01	0.08	-0.96	1.26	17.51	16.32	17.34	17.53	25.64	0.15	0.23	0.19	0.11	0.02
March	-0.28	-0.22	-0.15	-1.26	-0.25	13.13	12.30	12.87	14.44	17.14	0.44	0.59	0.51	0.33	0.32
April	-0.62	-0.38	-0.41	-0.53	-0.58	10.31	9.19	9.58	11.00	14.91	0.56	0.71	0.66	0.49	0.31
May	-1.07	-0.59	-0.60	-1.94	-1.56	23.18	21.16	22.89	23.27	34.19	0.18	0.29	0.25	0.15	0.01
June	-0.92	-0.87	-0.94	-1.19	-0.81	22.13	21.98	22.04	22.21	32.50	0.52	0.66	0.61	0.57	0.30
July	-1.94	-1.36	-2.01	-3.53	-2.09	23.16	22.89	22.92	23.01	31.35	0.62	0.68	0.65	0.64	0.44
August	-0.94	-0.92	-1.05	-1.35	-1.16	22.24	21.92	21.97	22.27	30.01	0.66	0.70	0.68	0.68	0.49
September	-0.62	-0.55	-0.62	-0.46	-0.87	20.39	20.01	20.08	20.44	28.12	0.50	0.57	0.54	0.56	0.32
October	-0.53	-0.31	-0.35	-0.63	-0.41	19.37	17.65	19.01	19.64	26.24	0.23	0.39	0.32	0.19	0.04
November	0.01	-0.33	-0.05	0.18	0.30	10.52	9.37	9.48	12.17	11.61	0.73	0.80	0.78	0.65	0.70
December	-0.27	-0.21	-0.11	-0.41	-0.22	9.67	8.59	9.12	10.82	10.83	0.63	0.71	0.69	0.54	0.61
Average	-0.64	-0.53	-0.54	-1.15	-0.63	17.42	16.15	16.65	17.54	23.41	0.47	0.57	0.53	0.44	0.31

Note. IDW = inverse distance weighting; KED = kriging with an external drift; MBE = mean bias error; OCK = ordinary cokriging; OK = ordinary kriging; R2 = coefficient of determination; RBF = radial basis function; RMSE = root mean square error.

RBF methods, the average R^2 values (Table 6) for the Middle Yarra River catchment are .53, .67, .62, .49 and .54, respectively whereas the average R^2 values for the Ovens River catchment are .47, .57, .53, .44, and .31, respectively. The higher R^2 value in the OCK and KED methods indicate that using elevation as a secondary variable brings more information in the rainfall estimation process under the kriging-based geostatistical analysis framework.

As explained by Delbari et al. (2013), using elevation as a secondary variable may not always improve the prediction accuracy through the OCK analysis if the spatial continuity of elevation is weaker than that of rainfall despite a high correlation exists between rainfall and elevation. In this study, the relative nugget effect (i.e., ratio of nugget coefficient to sill) of the direct variogram models for rainfall (Table 3) and elevation (Figure 5), and the cross-variogram models for rainfall-elevation (Table 4) for both the catchments are found very small in all months. This results in the improvement in the rainfall estimation by the OCK method, which is thus selected as the best interpolator for the study area in this study. Therefore, the OCK method (the best interpolator) is used to generate a continuous rainfall dataset of the monthly average rainfall for each of the catchments, which are shown in Figure 8 and Figure 9. The created datasets are expected to be very useful in various hydrological and water resources planning studies within the Yarra River catchment and the Ovens River catchment in Australia.

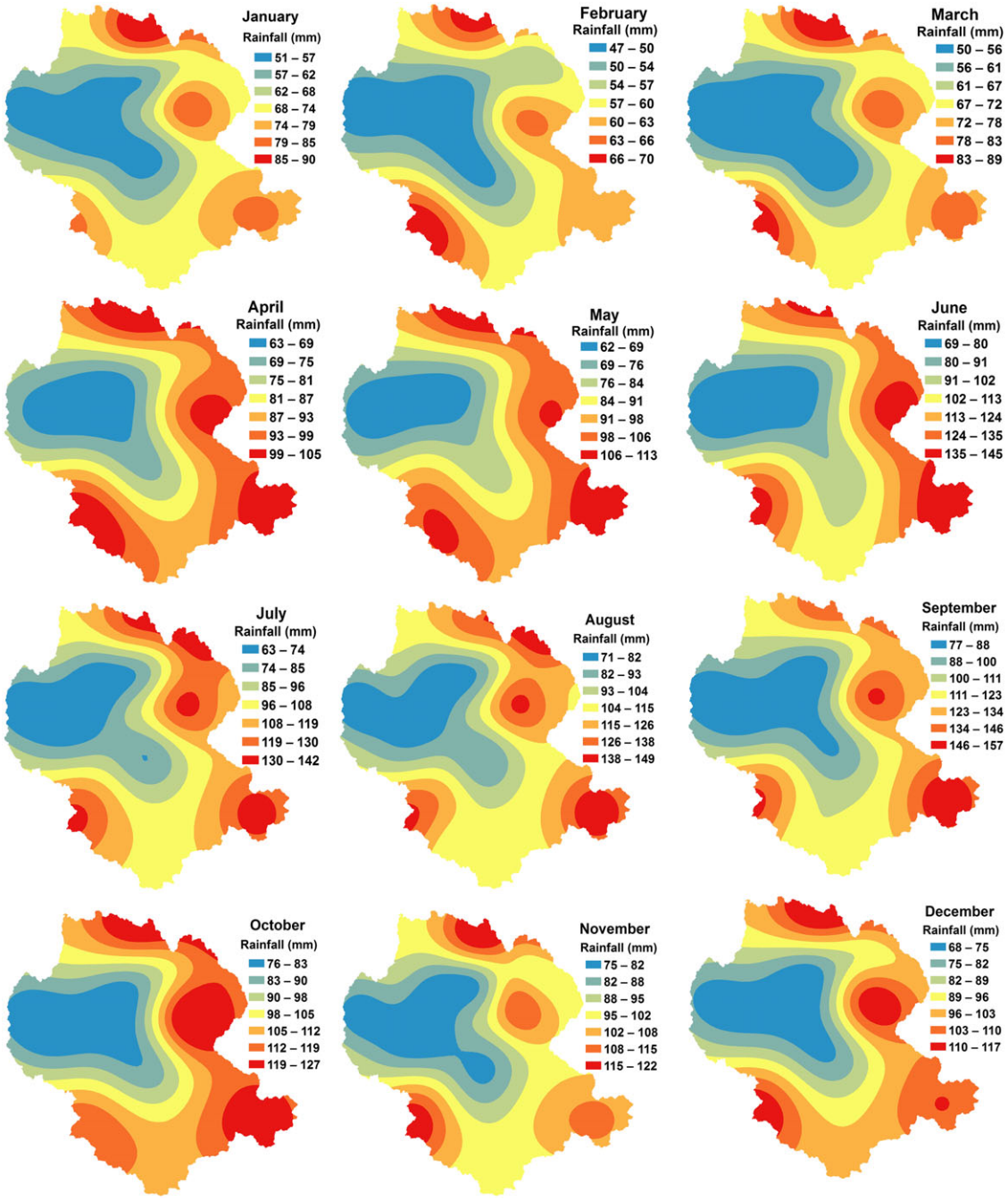

FIGURE 8 Spatial distribution of monthly rainfall in the Middle Yarra River catchment using the ordinary cokriging (the best interpolator in this study) interpolation method

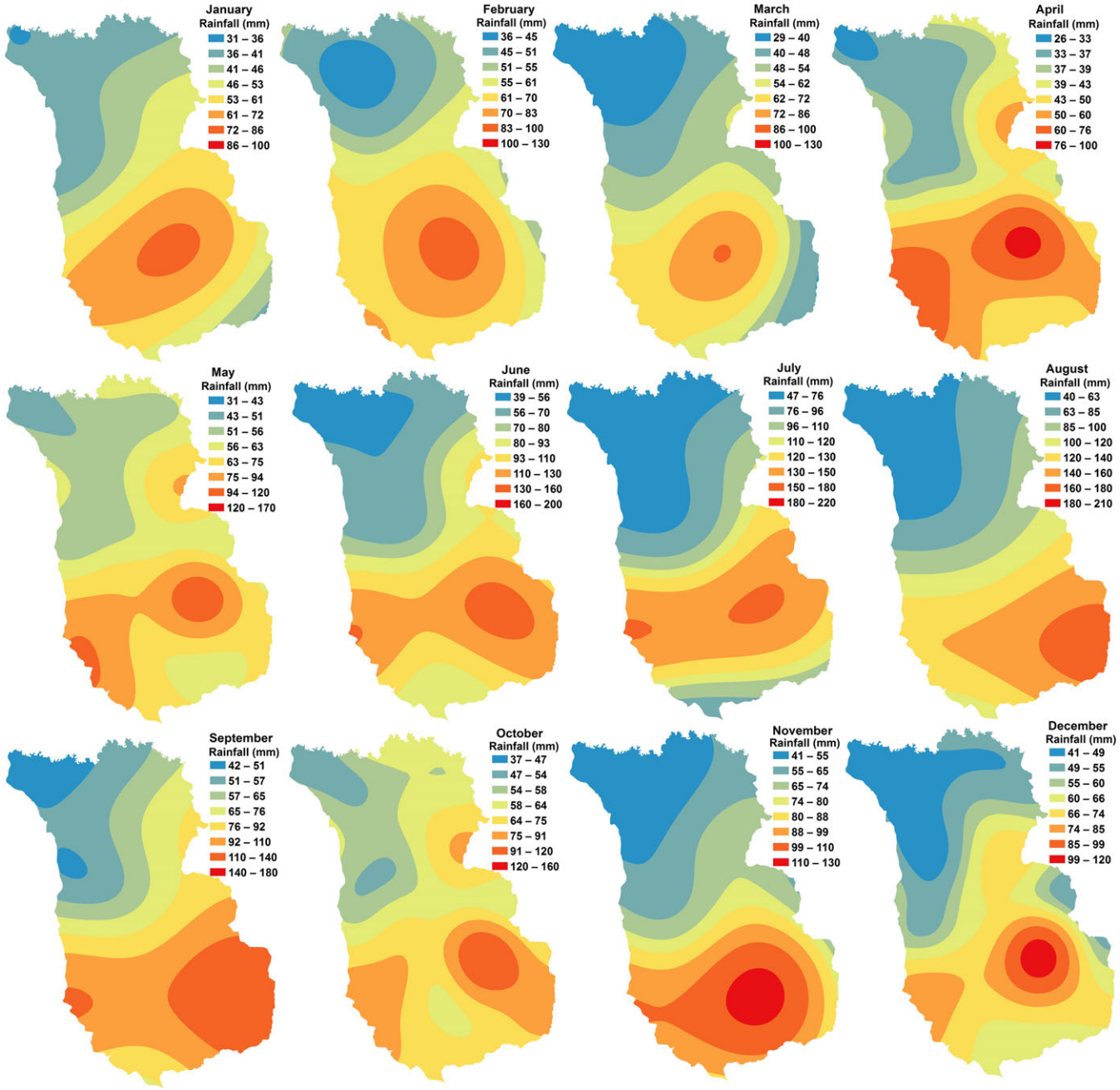

FIGURE 9 Spatial distribution of monthly rainfall in the Ovens River catchment using the ordinary cokriging (the best interpolator in this study) interpolation method

5 | CONCLUSIONS

In this study, three kriging-based geostatistical (OK, OCK, and KED) and two deterministic (IDW and RBF with thin plate spline) interpolation methods are used for estimating spatial distribution of monthly mean rainfall in the Middle Yarra River catchment and the Ovens River catchment in Victoria, Australia. The objective is to compare the performances of these interpolation methods to select the best interpolation method for generating a high quality continuous rainfall dataset in the form of a rainfall map for the study area. The elevation data obtained from a DEM of the study area is used as a supplementary variable in addition to rainfall records for the cokriging analysis using the ordinary cokriging and kriging with an external drift methods. Results show that the geostatistical methods outperform the deterministic methods for spatial interpolation of rainfall over the study area. Specifically, the performance of the cokriging methods (OCK and KED) is better than that of other geostatistical methods. The performance of the RBF with thin plate spline is found practically as good as the ordinary kriging method for rainfall estimation, whereas the IDW method is shown to have the worst results for the study area. OCK performs the best among all the interpolators and gives the improved estimates of rainfall in all months for both the catchments. It provides the lowest estimation errors and the highest correlations between the estimated and observed monthly average rainfall. Thus, ordinary cokriging is identified as the best interpolator in this study for estimating spatial distribution of rainfall in both the catchments. The obtained results

indicate that making use of elevation as an auxiliary variable in addition to rainfall data can enhance the estimation of rainfall in a catchment with the mountainous and/or complex terrain. This study thus recommends the use of cokriging for the generation of continuous rainfall map especially in catchments with high spatial variation of rainfall as well as elevation.

ACKNOWLEDGEMENTS

The authors acknowledge the financial support for this study through an International Postgraduate Research Scholarship (IPRS) provided by the Government of Australia and Victoria University, Melbourne. The authors are thankful to the Australian Bureau of Meteorology (BoM) and Geoscience Australia for providing the necessary data used in this study. The authors also wish to thank the Editor and three anonymous reviewers for their valuable comments and suggestions, which have improved the quality of this paper.

REFERENCES

Adhikary, S. K., Yilmaz, A. G., & Muttil, N. (2015). Optimal design of rain-gauge network in the Middle Yarra River catchment, Australia. *Hydrological Processes*, *29*(11), 2582–2599. https://doi.org/10.1002/hyp.10389

Adhikary, S. K., Muttil, N., & Yilmaz, A. G. (2016a). Ordinary kriging and genetic programming for spatial estimation of rainfall in the Middle Yarra River catchment, Australia. *Hydrology Research*, *47*(6), 1182–1197. https://doi.org/10.2166/nh.2016.196

Adhikary, S. K., Muttil, N., & Yilmaz, A. G. (2016b). Genetic programming-based ordinary kriging for spatial interpolation of rainfall. *Journal of Hydrologic Engineering*, *21*(2) 04015062. https://doi.org/10.1061/(ASCE)HE.1943-5584.0001300

ASCE (1996). *Hydrology handbook* (2nd ed.). American Society of Civil Engineers (ASCE): Reston, VA.

Barua, S., Muttil, N., Ng, A. W. M., & Perera, B. J. C. (2012). Rainfall trend and its implications for water resource management within the Yarra River catchment, Australia. *Hydrological Processes*, *27*(12), 1727–1738. https://doi.org/10.1002/hyp.9311

Boer, E. P. J., de Beurs, K. M., & Hartkamp, A. D. (2001). Kriging and thin plate splines for mapping climate variables. *International Journal of Applied Earth Observation and Geoinformation*, *3*(2), 146–154. https://doi.org/10.1016/S0303-2434(01)85006-6

Chen, F. W., & Liu, C. W. (2012). Estimation of the spatial rainfall distribution using inverse distance weighting (IDW) in the middle of Taiwan. *Paddy and Water Environment*, *10*(3), 209–222. https://doi.org/10.1007/s10333-012-0319-1

Chilès, J. P., & Delfiner, P. (1999). *Geostatistics: modeling spatial uncertainty*. New York: John Wiley & Sons.

Daly, C. (2006). Guidelines for assessing the suitability of spatial climate data sets. *International Journal of Climatology*, *26*(6), 707–721. https://doi.org/10.1002/joc.1322

Daly, E., Kolotelo, P., Schang, C., Osborne, C. A., Coleman, R., Deletic, A., & McCarthy, D. T. (2013). *Escherichia coli* Concentrations and loads in an urbanised catchment: The Yarra River, Australia. *Journal of Hydrology*, *497*, 51–61. https://doi.org/10.1016/j.jhydrol.2013.05.024

Delbari, M., Afrasiab, P., & Jahani, S. (2013). Spatial interpolation of monthly and annual rainfall in northeast of Iran. *Meteorology and Atmospheric Physics*, *122*(1), 103–113. https://doi.org/10.1007/s00703-013-0273-5

Di Piazza, A., Conti, F. L., Noto, L. V., Viola, F., & Loggia, G. L. (2011). Comparative analysis of different techniques for spatial interpolation of rainfall data to create a serially complete monthly time series of precipitation for Sicily, Italy. *International Journal of Applied Earth Observation and Geoinformation*, *13*(3), 396–408. https://doi.org/10.1016/j.jag.2011.01.005

Dirks, K. N., Hay, J. E., Stow, C. D., & Harris, D. (1998). High resolution studies of rainfall on Norfolk Island part II: Interpolation of rainfall data. *Journal of Hydrology*, *208*(3–4), 187–193. https://doi.org/10.1016/S0022-1694(98)00155-3

EPA Victoria. (2003). Environmental condition of rivers and streams in the Ovens catchment. Environment Report of EPA Victoria, Publication No. 909. Available at: <http://www.epa.vic.gov.au/~/media/Publications/909.pdf> (Accessed on: 20 November, 2016).

ESRI (2009). *ArcGISv9.3.1 (computer software product of ESRI)*. Redlands, CA, USA: Environmental Systems Research Institute (ESRI).

Feki, H., Slimani, M., & Cudennec, C. (2012). Incorporating elevation in rainfall interpolation in Tunisia using geostatistical methods. *Hydrological Sciences Journal*, *57*(7), 1294–1314. https://doi.org/10.1080/02626667.2012.710334

Gittins, R. (1968). Trend surface analysis of ecological data. *Journal of Ecology*, *56*(3), 845–869. https://doi.org/10.2307/2258110

Goovaerts, P. (1997). *Geostatistics for natural resources evaluation*. New York: Oxford University Press.

Goovaerts, P. (1999). Geostatistics in soil science: State-of-the-art and perspectives. *Geoderma*, *89*, 1–46. https://doi.org/10.1016/S0016-7061(98)00078-0

Goovaerts, P. (2000). Geostatistical approaches for incorporating elevation into the spatial interpolation of rainfall. *Journal of Hydrology*, *228*(1–2), 113–129. https://doi.org/10.1016/S0022-1694(00)00144-X

Gyasi-Agyei, Y. (2016). Assessment of radar-based locally varying anisotropy on daily rainfall interpolation. *Hydrological Sciences Journal*, *61*(10), 1890–1902. https://doi.org/10.1080/02626667.2015.1083652

Haddad, K., Rahman, A., Zaman, M., & Shrestha, S. (2013). Applicability of Monte Carlo cross validation technique for model development and validation using generalized least squares regression. *Journal of Hydrology*, *482*, 119–128. https://doi.org/10.1016/j.jhydrol.2012.12.041

Hancock, P. A., & Hutchinson, M. F. (2006). Spatial interpolation of large climate data sets using bivariate thin plate smoothing splines. *Environmental Modelling & Software*, *21*(12), 1684–1694. https://doi.org/10.1016/j.envsoft.2005.08.005

Hevesi, J. A., Istok, J. D., & Flint, A. L. (1992). Precipitation estimation in mountainous terrain using multivariate geostatistics (part 1 and 2). *Journal of Applied Meteorology*, *31*(7), 661–688. https://doi.org/10.1175/1520-0450(1992)031<0661:PEIMTU>2.0.CO;

Hsieh, H. H., Cheng, S. J., Liou, J. Y., Chou, S. C., & Siao, B. R. (2006). Characterization of spatially distributed summer daily rainfall. *Journal of Chinese Agricultural Engineering*, *52*, 47–55.

Hutchinson, M. F. (1995). Interpolating mean rainfall using thin plate smoothing splines. *International Journal of Geographical Information Systems*, *9*(4), 385–403. https://doi.org/10.1080/02693799508902045

Isaaks, H. E., & Srivastava, R. M. (1989). *Applied geostatistics*. New York: Oxford University Press.

Jeffrey, S. J., Carter, J. O., Moodie, K. B., & Beswick, A. R. (2001). Using spatial interpolation to construct a comprehensive archive of Australian climate data. *Environmental Modelling & Software*, *16*(4), 309–330. https://doi.org/10.1016/S1364-8152(01)00008-1

Johnson, F., Hutchinson, M. F., The C, Beesley, C., & Green, J. (2016). Topographic relationships for design rainfalls over Australia. *Journal of Hydrology*, *533*, 439–451. https://doi.org/10.1016/j.jhydrol.2015.12.035

Johnston, K., VerHoef, J. M., Krivoruchko, K., & Lucas, N. (2001). *Using ArcGIS geostatistical analyst*. Redlands, CA, USA: ArcGIS Manual by ESRI.

Jones, D. A., Wang, W., & Fawcett, R. (2009). High-quality spatial climate data-sets for Australia. *Australian Meteorological and Oceanographic Journal*, *58*(4), 233–248.

Journel, A., & Huijbregts, C. (1978). *Mining geostatistics*. New York: Academic Press.

Li, J., & Heap, A. D. (2011). A review of comparative studies of spatial interpolation methods in environmental sciences: Performance and impact factors. *Ecological Informatics*, *6*(3–4), 228–241. https://doi.org/10.1016/j.ecoinf.2010.12.003

Li, M., & Shao, Q. (2010). An improved statistical approach to merge satellite rainfall estimates and rain-gauge data. *Journal of Hydrology*, *385*(1–2), 51–64. https://doi.org/10.1016/j.jhydrol.2010.01.023

Lloyd, C. D. (2005). Assessing the effect of integrating elevation data into the estimation of monthly precipitation in Great Britain. *Journal of Hydrology*, *308*(1–4), 128–150. https://doi.org/10.1016/j.jhydrol.2004.10.026

Ly, S., Charles, C., & Degré, A. (2011). Geostatistical interpolation of daily rainfall at catchment scale: The use of several variogram models in the Ourthe and Ambleve catchments, Belgium. *Hydrology and Earth System Sciences*, *15*(7), 2259–2274. https://doi.org/10.5194/hess-15-2259-2011

Mair, A., & Fares, A. (2011). Comparison of rainfall interpolation methods in a mountainous region of a tropical island. *Journal of Hydrologic Engineering*, *16*(4), 371–383. https://doi.org/10.1061/(ASCE)HE.1943-5584.0000330

Martínez-cob, A. (1996). Multivariate geostatistical analysis of evapotranspiration and precipitation in mountainous terrain. *Journal of Hydrology*, *174*(1–2), 19–35. https://doi.org/10.1016/0022-1694(95)02755-6

Melbourne Water. (2015). Port Phillip and Westernport Regional River health strategy: Yarra catchment. Available at: <http://melbournewater.com.au/aboutus/reportsandpublications/key-strategies/Documents/Port%20Phillip%20and%20Westernport%20Regional%20River%20Health%20Strategy%20-%20Yarra%20catchment.pdf> (Accessed on: 20 October, 2015).

Moral, F. J. (2010). Comparison of different geostatistical approaches to map climate variables: Application to precipitation. *International Journal of Climatology*, *30*(4), 620–631. https://doi.org/10.1002/joc.1913

Phillips, D. L., Dolph, J., & Marks, D. (1992). A comparison of geostatistical procedures for spatial analysis of precipitation in mountainous terrain. *Agricultural and Forest Meteorology*, *58*(1–2), 119–141. https://doi.org/10.1016/0168-1923(92)90114-J

Robertson, G. P. (2008). *GS+: geostatistics for the environmental sciences*. Gamma Design Software: Plainwell, Michigan, USA.

Schreider, S. Y., Jakeman, A. J., Pittock, A. B., & Whetton, P. H. (1996). Estimation of possible climate change impacts on water availability, extreme flow events and soil moisture in the Goulburn and ovens basins, Victoria. *Climate Change*, *34*(3–4), 513–546. https://doi.org/10.1007/BF00139304

Sharma, R. H., & Shakya, N. M. (2006). Hydrological changes and its impact on water resources of Bagmati watershed, Nepal. *Journal of Hydrology*, *327*(3–4), 315–322. https://doi.org/10.1016/j.jhydrol.2005.11.051

Subyani, A. M., & Al-Dakheel, A. M. (2009). Multivariate geostatistical methods of mean annual and seasonal rainfall in Southwest Saudi Arabia. *Arabian Journal of Geosciences*, *2*(1), 19–27. https://doi.org/10.1007/s12517-008-0015-z

Teegavarapu, R. S. V., & Chandramouli, V. (2005). Improved weighting methods, deterministic and stochastic data-driven models for estimation of missing precipitation records. *Journal of Hydrology*, *312*(1–4), 191–206. https://doi.org/10.1016/j.jhydrol.2005.02.015

Thiessen, A. H. (1911). Precipitation averages for large areas. *Monthly Weather Review*, *39*(7), 1082–1084. https://doi.org/10.1175/1520-0493(1911)39<1082b:PAFLA>2.0.CO;2

Wackernagel, H. (2003). *Multivariate geostatistics: An introduction with applications* (3rd ed.). Berlin: Springer-Verlag.

Webster, R., & Oliver, M. A. (2007). *Geostatistics for environmental scientists* (2nd ed.). Chichester, United Kingdom: John Wiley & Sons.

Woldemeskel, F. M., Sivakumar, B., & Sharma, A. (2013). Merging gauge and satellite rainfall with specification of associated uncertainty across Australia. *Journal of Hydrology*, *499*, 167–176. https://doi.org/10.1016/j.jhydrol.2013.06.039

Yang, X., Xie, X., Liu, D. L., Ji, F., & Wang, L. (2015). Spatial interpolation of daily rainfall data for local climate impact assessment over greater Sydney region. *Advances in Meteorology*, *2015*, 563629. https://doi.org/10.1155/2015/563629

Yilmaz, A. G., & Perera, B. J. C. (2014). Extreme rainfall nonstationarity investigation and intensity–frequency–duration relationship. *Journal of Hydrologic Engineering*, *19*(6), 1160–1172. https://doi.org/10.1061/(ASCE)HE.1943-5584.0000878

Yilmaz, A. G., Hossain, I., & Perera, B. J. C. (2014). Effect of climate change and variability on extreme rainfall intensity–frequency–duration relationships: A case study of Melbourne. *Hydrology and Earth System Sciences*, *18*, 4065–4076. https://doi.org/10.5194/hess-18-4065-2014

Yu, M. C. L., Cartwright, I., Braden, J. L., & de Bree, S. T. (2013). Examining the spatial and temporal variation of groundwater inflows to a valley-to-floodplain river using 222Rn, geochemistry and river discharge: The Ovens River, Southeast Australia. *Hydrology and Earth System Sciences*, *17*(12), 4907–4924. https://doi.org/10.5194/hess-17-4907-2013

How to cite this article: Adhikary SK, Muttil N, Yilmaz AG. Cokriging for enhanced spatial interpolation of rainfall in two Australian catchments. *Hydrological Processes*. 2017;31:2143–2161. https://doi.org/10.1002/hyp.11163